ISA Transactions 142 (2023) 148–163

Contents lists available at ScienceDirect

ISA Transactions

journal homepage: www.elsevier.com/locate/isatrans

Research article

Modified Active Disturbance Rejection Predictive Control: A fixed-order state–space formulation for SISO systems

Blanca Viviana Martínez Carvajal *, Javier Sanchis Sáez, Sergio García-Nieto Rodríguez, Miguel Martínez Iranzo

Instituto Universitario de Automática e Informática Industrial, Universitat Politècnica de València, València, 46022, Spain

ARTICLE INFO

Article history:
Received 27 July 2022
Received in revised form 10 August 2023
Accepted 10 August 2023
Available online 21 August 2023

MSC:
00-01
99-00

Keywords:
Active Disturbance Rejection Control
Model Predictive Control
Constrained systems
State space model
Extended State Observer

ABSTRACT

This paper presents a novel control strategy that provides active disturbance rejection predictive control on constrained systems with no nominal identified model. The proposed loop relaxes the modelling requirement to a fixed discrete-time state–space realisation of a first-order plus integrator plant despite the nature of the controlled process. A third-order discrete Extended State Observer (ESO) estimates the model mismatch and assumed plant states. Moreover, the constraints handling is tackled by incorporating the compensation term related to the total perturbation in the definition of the optimisation problem constraints. The proposal merges in a new way state–space Model Predictive Control (MPC) and Active Disturbance Rejection Control (ADRC) into an architecture suitable for the servo-regulatory operation of linear and non-linear systems, as shown through validation examples.

1. Introduction

Model Predictive Control (MPC) is a set of advanced control techniques whose ability to predict the process behaviour while operating within active constraints makes it stand out among other control methods. To compute future outputs over a prediction horizon, an assumed trajectory of current and unknown future inputs is applied to an explicit internal model considered a proper representation of the real system; the goal is then to choose the input trajectory such that the output reaches the desired value at the end of that prediction horizon. The proper inputs are selected by solving an optimisation problem dependent on predictions, the measured output, and subject to desired constraints. Once the input trajectory is obtained, only the first of its elements is applied to the plant, and the whole procedure is repeated at the next instant when a new output measurement is available. This is known as the receding horizon strategy, represented in Fig. 1. It is argued that MPC is a satisfactory approach for a variety of problems [1] and an impactful technology in practice [2]. However, the need for a precise prediction model is still considered its main shortcoming [3].

Conversely, Active Disturbance Rejection Control (ADRC) [4,5] is a control technique that brings to discussion the challenging idea that a process, whether linear or non-linear, can be controlled without needing a detailed model of its functioning by approximating its dynamics to an integrator chain, commonly denoted as the modified plant. To achieve this, ADRC relies on an Extended State Observer (ESO), which provides information about the integrator states and the total perturbation (total disturbance): the total effect of the multiple disturbances that produce a difference between the actual plant and the assumed integrator chain [6]. The manipulated variable is then proportional to the result of adding the estimated total perturbation to a state feedback control law governing the assumed integrator chain, as shown in Fig. 2. The ADRC ability to deal with uncertainty and non-modelled dynamics has been evidenced in successful industrial applications such as thermal power plants [7], DC–DC buck converters [8] and robotic systems [9].

The rapid growth of ADRC has inspired works intended to integrate it with other control methods. This is considered an open area of research with two identified approaches. On the one hand, there is the ESO-based control in which a nominal state–space model of the process to be controlled is used to design a General ESO (GESO) [10]. For example, in [11], the GESO is discretised and used to update the dynamics of a prediction model

* Correspondence to: Instituto Universitario de Automática e Informática Industrial, Universitat Politècnica de València, Camino de Vera s/n, Building 5C, València 46022, Spain.

E-mail addresses: blamarca@doctor.upv.es (B.V. Martínez Carvajal), jsanchis@isa.upv.es (J. Sanchis Sáez), sgnieto@isa.upv.es (S. García-Nieto Rodríguez), mmiranzo@isa.upv.es (M. Martínez Iranzo).

https://doi.org/10.1016/j.isatra.2023.08.011

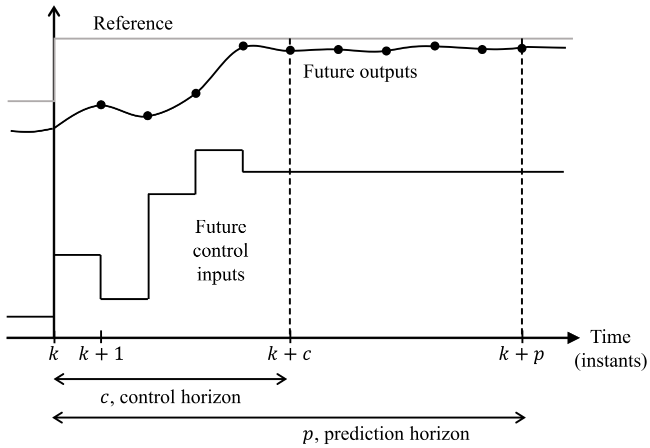

Fig. 1. Receding horizon strategy of model predictive control.

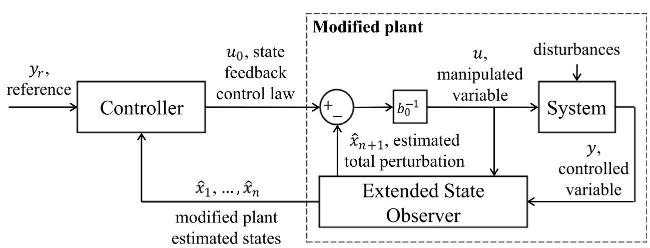

Fig. 2. Active disturbance rejection control loop.

to control the system state trajectories. More recently, in [12], the stability of the predictive ESO-based control is studied when the discrete GESO is employed as part of a predictive control problem that penalises the deviations of state predictions from zero. The above contributions have exploited the ESO structure by augmenting the state vector with states corresponding to disturbances. However, these implementations still require an identified nominal model of the process which turns into the standard approach of the disturbance observer-based control as those also proposed in [13,14], and [15].

On the other hand, there are works where the modified plant concept has been combined with the prediction strategy. For example, in [16], the output voltage of a DC–DC buck converter is rearranged as a function of total perturbation and an unconstrained continuous-time predictive control is designed. A reduced-order Generalized Proportional Integral Observer (GPIO) is implemented as the prediction model requires output and total perturbation derivatives. Even though this continuous configuration is analogous to the discrete-time MPC, some simplification should be made to truncate the number of higher-order derivatives and a discretisation of the control algorithm is needed to apply the input to the plant. In [17], the ESO estimates the external disturbances and modelling errors that arise from obtaining a lateral vehicle model for the steering control of a two-wheel vehicle. In this work, a constrained predictive control law is computed and modified with the compensation term to calculate the manipulated variable. However, the upper limit of the control action constraint in the optimisation problem is set as the upper limit of the real manipulated variable. With this definition, the control action computed during optimisation will likely be within the constraint band. Still, the manipulated variable applied to the actual system could evolve to a value outside the allowed limits due to the compensation term.

From another point of view, in [18–20], the discrete transfer function of the nth-order integrator is employed as a prediction model in a Generalized Predictive Controller (GPC), and the ESO is in charge of estimating the total perturbation that is further compensated in the loop. Although these proposals resemble a combination of the ADRC with an MPC method, none addresses the definition of constraints and the possible influence of the compensation term in their handling.

According to the findings presented in previous literature, the integration of ADRC with MPC methods offers potential performance and disturbance rejection benefits. Still, the following are identified as current research challenges: how to tap the disturbance estimation–rejection mechanism of ADRC to reject the ignored dynamics actively and thus avoid the modelling effort imposed on MPC, how to incorporate the disturbance compensation term in the MPC optimisation problem definition to ensure that the manipulated variable satisfies the absolute operating limits in servo-regulatory operation, and to what extent the integration of MPC and ADRC frameworks allows obtaining the desired performance for different types of systems. In this sense, the significant contribution of this work is a novel control architecture that provides predictive control on systems with no nominal identified model and that are subject to operational constraints in output, the magnitude of input, and its increment. The above is achieved by using the disturbance rejection mechanism of the ADRC to enforce the controlled plant to behave like a first-order plus integrator model governed by an optimal control law computed by predicting the output of this assumed plant over a horizon and according to the allowed constraints. The proposed loop is implemented as a discrete-time algorithm different from previously published works mainly because of the following highlights.

- The estimation–rejection mechanism of the ADRC as an internal loop is maintained to enforce the plant dynamics to behave like a disturbance-free modified plant. Consequently, the predictive control problem is solved based on a fixed discrete state space model of second-order resembling a first-order plus integrator realisation, despite the nature of the controlled system. Moreover, conditions for the feasibility of the optimisation problem and the nominal stability are given.
- The modelling requirements on the controlled plant are reduced to natural system characteristics such as static gain and apparent time constant due to the ADRC estimation–rejection mechanism. Therefore, the model-based feature of predictive control is relaxed, and the need for the detailed identification of the system is eliminated.
- The proposed control structure allows the constraints handling. Specifically, the compensation term resulting from the total perturbation estimation is included in the definition of the optimisation problem constraints. Thus, the operation ranges related to the output, the magnitude of input and its rate of change are directly considered. The above prevents the violation of the input constraint after the predictive control law is compensated in the loop.
- The proposed scheme is suitable for the control of processes with complex dynamics. To study the challenging scenario of meeting performance requirements when a relaxation in modelling has been assumed, the servo-regulatory performance of the proposed strategy is evaluated when controlling constrained linear and non-linear benchmark systems with uncertainty and external perturbations.

The remaining structure of this paper is organised as follows. In Section 2, state–space MPC and linear ADRC (LADRC) are briefly described as preliminaries to Section 3, where the proposed modified closed loop with active disturbance rejection and output predictions is explained in detail. The proposal is validated in

Section 4 with the control of linear benchmark systems. The validation is then expanded to a non-linear benchmark, considering as a case study the Continuous Stirred Tank Reactor (CSTR). Finally, conclusions and future work are drawn in Section 5.

2. State–space MPC and discrete LADRC formulations

MPC is an entirely discrete algorithm, whereas LADRC has its theoretical formulation in the continuous-time domain. However, the practical implementation of LADRC requires a discretisation of its main comprising block: the ESO. Offset-free MPC and discrete LADRC for single-input single-output systems are briefly introduced in the following.

2.1. Offset-free model predictive control

Model Predictive Control refers to a set of advanced control methods in which the control action is computed based on predictions of the output behaviour, hence the importance of accurate modelling of the process to be controlled [1]. The most commonly used models are the step response (in Dynamic Matrix Control, DMC), the transfer function (in GPC), and the discrete state–space realisation of order n (1), where $\mathbf{x}_k \in \mathbb{R}^{n\times 1}$ is the state vector, $\boldsymbol{\nu} \in \mathbb{R}^{n\times 1}$ is a state disturbance vector, y is the controlled variable, u is the manipulated variable, and $A \in \mathbb{R}^{n\times n}$, $B \in \mathbb{R}^{n\times 1}$, and $C \in \mathbb{R}^{1\times n}$ are the system matrices.

$$\begin{aligned} \mathbf{x}_{k+1} &= A\mathbf{x}_k + Bu_k + \boldsymbol{\nu}_k \\ y_k &= C\mathbf{x}_k, \end{aligned} \tag{1}$$

The MPC algorithm solves for each instant k an optimisation problem that minimises the cost function (2), along a prediction horizon p, subject to none, some or all of the constraints (3)–(5). Notation $y_{f,i|k}$ indicates that future output at instant $k+i$ is calculated based on conditions at instant k; The same holds for the reference trajectory $y_{r,i|k}$ and the rate of input $\Delta u_{i|k} = u_{i|k} - u_{i-1}$. It is always assumed that the control horizon c satisfies $c \le p$ and that $\Delta u_{i|k} = 0$ for $i \ge c$. The cost function (2) considers the quadratic forms of the tracking error $\|y_{r,i|k} - y_{f,i|k}\|_\gamma^2$ and the rate of manipulated variable $\|\Delta u_{i|k}\|_\lambda^2$ with scaling factors γ and λ, respectively, and subject to the variables constrained between their allowed lower and upper limits represented by the bar notations $\underline{w}$ and $\overline{w}$, correspondingly.

$$J = \sum_{i=1}^{p} \|y_{r,i|k} - y_{f,i|k}\|_\gamma^2 + \sum_{i=0}^{c-1} \|\Delta u_{i|k}\|_\lambda^2 \tag{2}$$

$$\underline{\Delta u} \le \Delta u_{i|k} \le \overline{\Delta u}, \qquad i = 0, \dots, c-1, \tag{3}$$

$$\underline{u} \le u_{i|k} \le \bar{u}, \qquad i = 0, \dots, c-1, \tag{4}$$

$$\underline{y} \le y_{f,i|k} \le \bar{y}, \qquad i = 1, \dots, p. \tag{5}$$

When the discrete state–space model (1) is used to formulate the predictive control problem, the objective function (2) can be written as

$$J = \|\mathbf{y_r} - \mathbf{y_f}\|_\Gamma^2 + \|\boldsymbol{\Delta}\mathbf{u}\|_\Lambda^2, \tag{6}$$

with

$$\mathbf{y_r} = \left[y_{r,1|k}, y_{r,2|k}, \dots, y_{r,p|k}\right]^\top, \tag{7}$$

$$\mathbf{y_f} = \left[y_{f,1|k}, y_{f,2|k}, \dots, y_{f,p|k}\right]^\top, \tag{8}$$

$$\boldsymbol{\Delta}\mathbf{u} = \left[\Delta u_{0|k}, \Delta u_{1|k}, \dots, \Delta u_{c-1|k}\right]^\top, \tag{9}$$

$$\Gamma = \mathrm{diag}(\gamma) \in \mathbb{R}^{p\times p}, \tag{10}$$

$$\Lambda = \mathrm{diag}(\lambda) \in \mathbb{R}^{c\times c}. \tag{11}$$

In index (6), the deviation of p future outputs $\mathbf{y_f}$ from the reference trajectory $\mathbf{y_r}$ is penalised through the diagonal weighting matrix Γ. Likewise, penalisation of the actual and $c-1$ future control efforts $\boldsymbol{\Delta}\mathbf{u}$ is introduced using the matrix Λ. The output predictions are computed based on the current state (or an estimation of it), the last applied input, and the unknown actual and future input changes according to

$$\mathbf{y_f} = \underbrace{P\mathbf{x}_k + VBu_{k-1} + \mathbf{w}_k + V\boldsymbol{\nu}_k}_{\mathbf{y_{free}}} + G\boldsymbol{\Delta}\mathbf{u}, \tag{12}$$

where matrices $P \in \mathbb{R}^{p\times p}$, $V \in \mathbb{R}^{p\times 1}$, and $G \in \mathbb{R}^{p\times c}$ are obtained by using model (1) recursively along the prediction horizon. In addition, the correction term $\mathbf{w}_k \in \mathbb{R}^{p\times 1}$ and the state disturbance prediction model $\boldsymbol{\nu}_k \in \mathbb{R}^{p\times 1}$ are included in (12) to provide offset-free control (OF-MPC) [21].

When no constraints are imposed, the minimum of (6) can be directly calculated as a matrix product. However, when constraints are active, there is no explicit solution, and the standard approach is to treat the new problem as a quadratic one, which is easily handled by solvers like *quadprog* from Matlab or Mosek [22].

2.2. Discrete linear active disturbance rejection control

In contrast to OF-MPC, Linear Active Disturbance Rejection Control is a control algorithm based on the idea that a detailed process model is not necessary to control it. Instead, LADRC relies on input–output information to estimate the existing mismatch between the real system and an assumed integrator-chain modified plant used to design a linear state feedback control law.

For example, let (13) be the input–output representation of a second-order process with y as the controlled variable, u as the manipulated variable, a_0, a_1 as modelling coefficients, and b as a factor of the control action commonly known as critical gain.

$$\ddot{y} = -a_1\dot{y} - a_0 y + bu \tag{13}$$

The model (13) can be rearranged as (14) where it has been assumed that the only model information available is b_0, a nominal (approximated) value of the critical gain, and thus, the unknown and non-modelled dynamics is lumped in f denoted as total perturbation. Any external disturbances affecting the system are also accounted for as part of f.

$$\ddot{y} = b_0 u + f \tag{14}$$

A state–space representation of (14) is obtained by assigning the unknown total perturbation as a third state such that $\mathbf{x} = [x_1, x_2, x_3]^\top = [y, \dot{y}, f]^\top$ and, for discrete-time implementations, a discrete extended state observer must be used to estimate the state vector, preferably the current-observer configuration that offers improvement in terms of estimation accuracy and closed-loop stability compared to the predictive-observer [23].

In the current-ESO implementation, the estimated state vector $\hat{\mathbf{x}}_k$ is updated based on the measured output y_k according to

$$\hat{\mathbf{x}}_k = (A_L - \boldsymbol{\ell} C_L A_L)\,\hat{\mathbf{x}}_{k-1} + (B_L - \boldsymbol{\ell} C_L B_L)\,u_{k-1} + \boldsymbol{\ell} y_k, \tag{15}$$

where A_L, B_L, and C_L are the discrete version of the matrices from the continuous extended state–space model of (14) obtained through zero-order hold discretisation with sampling time T_s [24].

The vector $\boldsymbol{\ell} = [\ell_1, \ell_2, \ell_3]^\top$ in (15) represents the observer gains computed by equating the observer characteristic equation with the desired characteristic equation for the estimation error, as in (16). A common approach is to locate the three observer poles in the same position inside the unit circle $z_L = \exp(-\omega_o T_s)$, making the observer gains only dependent on its bandwidth, denoted by ω_o.

$$|zI - (A_L - \boldsymbol{\ell} C_L A_L)| = (z - z_L)^3. \tag{16}$$

Finally, the estimated state vector is used to compute the control law (17), with $y_{r,k}$ as the desired output value and ω_c as the controller bandwidth. Notice that, with an adequate design for the observer, each instant $\hat{x}_{3,k} \approx f$ and the total perturbation is eliminated from the system dynamics (14), allowing the closed-loop response to be governed by the law dependent on ω_c.

$$u_k = \frac{{\omega_c}^2 \left[y_{r,k} - \hat{x}_{1,k}\right] - 2\omega_c \hat{x}_{2,k} - \hat{x}_{3,k}}{b_0} \tag{17}$$

The combined action of estimating the disturbance information and compensating it from the loop through the manipulated variable is the core concept of LADRC. This disturbance rejection capability is performed by the *disturbance rejector*: the mechanism comprised of the ESO and the internal addition operation where the control law acting on the real plant is computed [25] (see Fig. 2). In this sense, the LADRC enforces the system to behave as a modified plant whose dynamics is used to design the observer and controlled by the state feedback law $u_{0,k} = {\omega_c}^2 \left[y_{r,k} - \hat{x}_{1,k}\right] - 2\omega_c \hat{x}_{2,k}$.

3. Constrained control loop with active disturbance rejection and output predictions

In the previous section, OF-MPC and LADRC were briefly described. Let the following comments about both algorithms be the introduction to this section.

On the one hand, if a proper model is available, OF-MPC becomes a robust algorithm with an optimal control action that satisfies the process constraints according to the optimisation problem feasibility. However, this model-based feature plays against the system performance when a significant model mismatch arises, for example, in processes with complex dynamics and different operating points.

On the other hand, LADRC locates itself almost on the opposite side of the spectrum by keeping the information required from modelling to a minimum and relying on its rejector mechanism to perform the disturbance rejection. Actually, this configuration offers proper control because it actively combines the non-modelled dynamics in an estimated state without the need for further knowledge. Nevertheless, some additional characteristic information about the system behaviour might be beneficial, resulting in an assumed plant different from the conventional integrator-chain form. What is more, some important control aspects, such as system constraints, mainly handled by limiters inside the loop, could be incorporated into a more dedicated control law.

To take advantage of the unique benefits of the mentioned control schemes whilst enhancing each other, the control architecture of Fig. 3 is proposed to merge the LADRC disturbance rejector and the receding horizon feature of MPC. Three main structures are identified:

① The system which corresponds to the real process to be controlled and whose precise mathematical model is unknown.

② The disturbance rejector representing the active disturbance rejection component of the loop. It is comprised of a current-ESO, intended for the proper estimation of system states and total perturbation, and the sum-gain configuration that uses the estimated total perturbation to compensate for the existing differences between the real plant and the modified plant. A general first-order plus integrator model is assumed as the modified plant. Therefore, the disturbance rejector is designed to overcome the possible structural and parametric mismatch as well as the external disturbances acting on the loop.

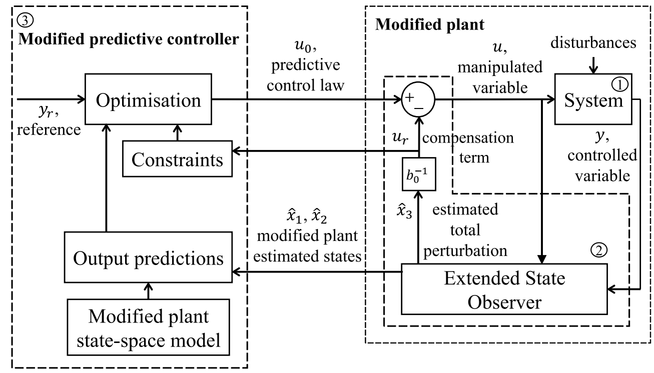

Fig. 3. Proposed control architecture. The system dynamics ① is enforced by the disturbance rejector ② into a first-order plus integrator plant (modified plant) governed by a modified predictive controller ③.

③ The modified predictive controller designed to provide a control law for the disturbance-free modified plant. This control law results from a constrained optimisation process where a cost function involving the tracking error and changes in input is minimised. By incorporating the predictive control algorithm into the loop, the receding horizon characteristic of this advanced control method is exploited in the servo-regulatory operation and constraints are directly taken into account.

The following subsections elaborate on the disturbance rejector and the modified predictive control functionalities.

3.1. Disturbance rejector

Let the first-order plus integrator model (18) represent the dynamics of the assumed modified plant into which the disturbance rejector is expected to enforce the real dynamics. The controlled variable is y, the manipulated variable is u, K represents the static gain, τ is the apparent time constant, and f is the total perturbation.

$$\ddot{y} = -\frac{1}{\tau}\dot{y} + \frac{K}{\tau}u + f \tag{18}$$

Selection of a first-order plus integrator system as modified plant mainly offers the following advantages: it constitutes a fixed mathematical representation of known order for the process to be controlled with a lower complexity involved in the identification of its parameters; It models the integral effect commonly present in industrial processes and approximate other types of dominant dynamics through a term with a time constant. Compared to the conventional chain-integrator form of LADRC, the additional dynamic information represented by the time constant enhances the estimation ability of the observer and increases the ESO efficiency [26].

A continuous-time state–space realisation of (18) is

$$\begin{bmatrix} \dot{x}_1 \\ \dot{x}_2 \end{bmatrix} = \begin{bmatrix} 0 & 1 \\ 0 & -1/\tau \end{bmatrix} \begin{bmatrix} x_1 \\ x_2 \end{bmatrix} + \begin{bmatrix} 0 \\ K/\tau \end{bmatrix} u + \begin{bmatrix} 0 \\ 1 \end{bmatrix} f \quad ;$$
$$y = \begin{bmatrix} 1 & 0 \end{bmatrix} \begin{bmatrix} x_1 \\ x_2 \end{bmatrix}. \tag{19}$$

If zero-order hold discretisation with sampling time T_s is used on (19), the discrete state–space model obtained is (20) with

$a = \exp(-T_s/\tau)$ and $b_0 = K/\tau$ as the nominal value of critical gain.

$$\begin{bmatrix} x_{1,k+1} \\ x_{2,k+1} \end{bmatrix} = \begin{bmatrix} 1 & \tau(1-a) \\ 0 & a \end{bmatrix} \begin{bmatrix} x_{1,k} \\ x_{2,k} \end{bmatrix} + b_0 \begin{bmatrix} \tau T_s - \tau^2(1-a) \\ \tau(1-a) \end{bmatrix} u_k + \begin{bmatrix} \tau T_s - \tau^2(1-a) \\ \tau(1-a) \end{bmatrix} f_k$$
$$y_k = \begin{bmatrix} 1 & 0 \end{bmatrix} \begin{bmatrix} x_{1,k} \\ x_{2,k} \end{bmatrix} \tag{20}$$

Assigning f_k to a third state, the extended state vector $\hat{\mathbf{x}}_k = [\hat{x}_{1,k}, \hat{x}_{2,k}, \hat{x}_{3,k}]^\top$ is updated according to (21), where the observer matrices A_o, B_o, and C_o are defined as (22).

$$\hat{\mathbf{x}}_k = (A_o - \boldsymbol{\ell}_o C_o A_o)\,\hat{\mathbf{x}}_{k-1} + (B_o - \boldsymbol{\ell}_o C_o B_o)\,u_{k-1} + \boldsymbol{\ell}_o y_k \tag{21}$$

$$A_o = \begin{bmatrix} 1 & \tau(1-a) & \tau T_s - \tau^2(1-a) \\ 0 & a & \tau(1-a) \\ 0 & 0 & 1 \end{bmatrix}$$
$$B_o = b_0 \begin{bmatrix} \tau T_s - \tau^2(1-a) \\ \tau(1-a) \\ 0 \end{bmatrix} \tag{22}$$
$$C_o = \begin{bmatrix} 1 & 0 & 0 \end{bmatrix}$$

Likewise, the observer gain vector $\boldsymbol{\ell}_o$ is determined based on the desired location of the observer poles inside the unit circle [24]. By following the same approach used in the design of conventional current-ESO, the corresponding gains are (23)–(25), with $z_o = \exp(-\omega_o T_s)$.

$$\ell_{o1} = 1 - \frac{z_o^3}{a}, \tag{23}$$

$$\ell_{o2} = \frac{2a - \ell_{o1}(1+a) + \ell_{o3}\left[\tau^2(1-a) - a\tau T_s\right] - 3z_o^2 + 1}{\tau(1-a)}, \tag{24}$$

$$\ell_{o3} = \frac{(1-z_o)^3}{\tau T_s(1-a)}, \tag{25}$$

Consequently, the design of the current-ESO in the proposed loop is dependent on the apparent time constant of modified plant τ, the sampling time T_s, and the desired bandwidth ω_o.

Let the control action affecting the system to be

$$u_k = u_{0,k} - \frac{\hat{x}_{3,k}}{b_0} \tag{26}$$

with $u_{0,k}$ denoting the value for instant k of a control action computed by a predictive control algorithm. If (26) is substituted in (20), it follows that

$$\begin{bmatrix} x_{1,k+1} \\ x_{2,k+1} \end{bmatrix} = \begin{bmatrix} 1 & \tau(1-a) \\ 0 & a \end{bmatrix} \begin{bmatrix} x_{1,k} \\ x_{2,k} \end{bmatrix} + b_0 \begin{bmatrix} \tau T_s - \tau^2(1-a) \\ \tau(1-a) \end{bmatrix} u_{0,k} - b_0 \begin{bmatrix} \tau T_s - \tau^2(1-a) \\ \tau(1-a) \end{bmatrix} \frac{\hat{x}_{3,k}}{b_0} + \begin{bmatrix} \tau T_s - \tau^2(1-a) \\ \tau(1-a) \end{bmatrix} f_k \tag{27}$$

and, under the premise that $\hat{x}_{3,k} \approx f_k$, the last two terms in the right-hand side of (27) cancel out, resulting in the disturbance-free modified plant.

$$\begin{bmatrix} x_{1,k+1} \\ x_{2,k+1} \end{bmatrix} = \underbrace{\begin{bmatrix} 1 & \tau(1-a) \\ 0 & a \end{bmatrix}}_{A} \underbrace{\begin{bmatrix} x_{1,k} \\ x_{2,k} \end{bmatrix}}_{\mathbf{x}_k} + \underbrace{b_0 \begin{bmatrix} \tau T_s - \tau^2(1-a) \\ \tau(1-a) \end{bmatrix}}_{B} u_{0,k} \tag{28}$$
$$y_k = \underbrace{\begin{bmatrix} 1 & 0 \end{bmatrix}}_{C} \begin{bmatrix} x_{1,k} \\ x_{2,k} \end{bmatrix}$$

Up to this point, it has been shown how the current-ESO estimates the modified plant states and the total perturbation. When the latter is used to compute the manipulated variable acting on the system, the model mismatch and external disturbances are compensated, allowing the discrete-time realisation of the first-order plus integrator system from (28) to be used as a prediction model to obtain the predictive control law $u_{0,k}$.

3.2. Modified predictive controller

Let J_M be the quadratic cost index associated with the optimisation problem of the modified predictive controller such that

$$J_M = \sum_{i=1}^{p} \|y_{r,i|k} - y_{f,i|k}\|_\gamma^2 + \sum_{i=0}^{c-1} \|\Delta u_{0,i|k}\|_\lambda^2, \tag{29}$$

which results in

$$J_M = \|\mathbf{y_r} - \mathbf{y_f}\|_\Gamma^2 + \|\boldsymbol{\Delta}\mathbf{u_0}\|_\Lambda^2 \tag{30}$$

with $\boldsymbol{\Delta}\mathbf{u_0} = \left[\Delta u_{0,0|k}, \Delta u_{0,1|k}, \ldots, \Delta u_{0,c-1|k}\right]^\top$ and $\mathbf{y_f}$ as the vector of p output predictions

$$\mathbf{y_f} = \underbrace{P\hat{\mathbf{x}}_k + VBu_{0,k-1}}_{\mathbf{y_{free}}} + G\boldsymbol{\Delta}\mathbf{u_0}. \tag{31}$$

Notice that neither the correction term nor the disturbance prediction model are included in (31). This is because the observer provides the current estimated state vector $\hat{\mathbf{x}}_k$ of the modified plant and consequently, matrices $P \in \mathbb{R}^{p\times 2}$, $V \in \mathbb{R}^{p\times 1}$, and $G \in \mathbb{R}^{p\times c}$ are computed using the discrete state–space realisation from (28).

In order to incorporate the real system constraints in the optimisation problem related to (29), the following formulation based on the classical Quadratic Dynamic Matrix Control (QDMC) approach is proposed.

Firstly, consider constrains on the manipulated variable specified as (4). For instant k, it holds that

$$u_{0|k} \le \overline{u}. \tag{32}$$

According to (26), $u_{0|k}$ can be rewritten as $u_{0|k} = \left[\Delta u_{0,0|k} + u_{0,k-1}\right] - (1/b_0)\hat{x}_{3,k}$ and substituting the latter in (32) leads to

$$\Delta u_{0,0|k} \le \overline{u} - u_{0,k-1} + \frac{\hat{x}_{3,k}}{b_0}. \tag{33}$$

Thus, the upper limit constraint on input magnitude $\overline{u}$ has been used to determine the corresponding upper limit constraint for the first decision variable of (30), $\Delta u_{0,0|k}$, taking into account the contribution of the disturbance rejector to the manipulated variable $u_{0|k}$.

The above procedure is expanded along the control horizon as follows.

$$\begin{aligned}
\Delta u_{0,1|k} + \Delta u_{0,0|k} &\leq \bar{u} - u_{0,k-1} + \frac{\hat{x}_{3,1|k}}{b_0} \\
\Delta u_{0,2|k} + \Delta u_{0,1|k} + \Delta u_{0,0|k} &\leq \bar{u} - u_{0,k-1} + \frac{\hat{x}_{3,2|k}}{b_0} \\
&\vdots \\
\Delta u_{0,c-1|k} + \cdots + \Delta u_{0,0|k} &\leq \bar{u} - u_{0,k-1} + \frac{\hat{x}_{3,c-1|k}}{b_0}
\end{aligned} \quad (34)$$

From Eq. (34) is evident that future values of the estimated total perturbation are required, which are not available. Still, it can be assumed that $\hat{x}_{3,k}$ remains constant over the control horizon and its value is updated by the ESO each time the optimisation problem needs to be solved. This is, $\hat{x}_{3,k} = \hat{x}_{3,1|k} = \cdots = \hat{x}_{3,c-1|k}$, and as a result

$$\begin{aligned}
\Delta u_{0,1|k} + \Delta u_{0,0|k} &\leq \bar{u} - u_{0,k-1} + \frac{\hat{x}_{3,k}}{b_0} \\
\Delta u_{0,2|k} + \Delta u_{0,1|k} + \Delta u_{0,k|k} &\leq \bar{u} - u_{0,k-1} + \frac{\hat{x}_{3,k}}{b_0} \\
&\vdots \\
\Delta u_{0,c-1|k} + \cdots + \Delta u_{0,0|k} &\leq \bar{u} - u_{0,k-1} + \frac{\hat{x}_{3,k}}{b_0}.
\end{aligned} \quad (35)$$

A similar development is done to determine the lower limit constraints on $\mathbf{\Delta u_0}$ as a function of the allowed lower limit $\underline{u}$ for the manipulated variable such that

$$\begin{aligned}
-\Delta u_{0,1|k} - \Delta u_{0,0|k} &\leq -\underline{u} + u_{0,k-1} - \frac{\hat{x}_{3,k}}{b_0} \\
-\Delta u_{0,2|k} - \Delta u_{0,1|k} - \Delta u_{0,0|k} &\leq -\underline{u} + u_{0,k-1} - \frac{\hat{x}_{3,k}}{b_0} \\
&\vdots \\
-\Delta u_{0,c-1|k} - \cdots - \Delta u_{0,0|k} &\leq -\underline{u} + u_{0,k-1} - \frac{\hat{x}_{3,k}}{b_0}.
\end{aligned} \quad (36)$$

Gathering inequalities from (35) and (36) results in the matrix form (37), where $I_L \in \mathbb{R}^{c\times c}$ is an all-ones lower triangular matrix; $\bar{\mathbf{u}} \in \mathbb{R}^{c\times 1}$ and $\underline{\mathbf{u}} \in \mathbb{R}^{c\times 1}$ are vectors of repeated elements $\bar{u}$ and $\underline{u}$, respectively; $\mathbf{1} \in \mathbb{R}^{c\times 1}$ is an all-ones vector, and $u_{r,k} = (1/b_0)\hat{x}_{3,k}$ represents the contribution of the disturbance rejector to the manipulated variable.

$$\underbrace{\begin{bmatrix} I_L \\ -I_L \end{bmatrix}}_{A_u} \underbrace{\begin{bmatrix} \Delta u_{0,0|k} \\ \Delta u_{0,1|k} \\ \vdots \\ \Delta u_{0,c-1|k} \end{bmatrix}}_{\mathbf{\Delta u_0}} \leq \underbrace{\begin{bmatrix} \bar{\mathbf{u}} \\ -\underline{\mathbf{u}} \end{bmatrix} - \begin{bmatrix} \mathbf{1} \\ -\mathbf{1} \end{bmatrix} u_{0,k-1} + \begin{bmatrix} \mathbf{1} \\ -\mathbf{1} \end{bmatrix} u_{r,k}}_{\mathbf{b_u}} \quad (37)$$

Attention is now drawn to the handling of constraints on the rate of change of input given in the form of (3). Proceeding as before, for instant k, it holds that

$$\begin{aligned}
\Delta u_{0|k} &\leq \overline{\Delta u} \\
u_{0|k} - u_{k-1} &\leq \overline{\Delta u}.
\end{aligned} \quad (38)$$

Using (26) in (38), it follows that

$$\left[\Delta u_{0,0|k} + u_{0,k-1} - \frac{\hat{x}_{3,k}}{b_0}\right] - u_{k-1} \leq \overline{\Delta u}. \quad (39)$$

Furthermore, $u_{k-1} = u_{0,k-1} - (1/b_0)\hat{x}_{3,k-1}$. Thus, substituting the latter in (39) and reorganising terms

$$\begin{aligned}
\Delta u_{0,0|k} &\leq \overline{\Delta u} - u_{0,k-1} + u_{0,k-1} + \frac{\hat{x}_{3,k}}{b_0} - \frac{\hat{x}_{3,k-1}}{b_0} \\
\Delta u_{0,0|k} &\leq \overline{\Delta u} + \frac{\hat{x}_{3,k}}{b_0} - \frac{\hat{x}_{3,k-1}}{b_0} \\
\Delta u_{0,0|k} &\leq \overline{\Delta u} + \frac{\Delta\hat{x}_{3,k}}{b_0}.
\end{aligned} \quad (40)$$

Likewise, for future control moves, constraints become

$$\begin{aligned}
\Delta u_{0,1|k} &\leq \overline{\Delta u} + \frac{\Delta\hat{x}_{3,1|k}}{b_0} \\
\Delta u_{0,2|k} &\leq \overline{\Delta u} + \frac{\Delta\hat{x}_{3,2|k}}{b_0} \\
&\vdots \\
\Delta u_{0,c-1|k} &\leq \overline{\Delta u} + \frac{\Delta\hat{x}_{3,c-1|k}}{b_0}.
\end{aligned} \quad (41)$$

However, as it was assumed that $x_{3,k}$ remains constant along the control horizon, $\Delta\hat{x}_{3,1|k} = \Delta\hat{x}_{3,2|k} = \cdots = \Delta\hat{x}_{3,c-1|k} = 0$, indicating that the disturbance rejector contribution to the manipulated variable is only affecting the constraint on the first decision variable $\Delta u_{0,0|k}$.

Constraints for the lower bound of $\mathbf{\Delta u_0}$ based on $\underline{\Delta u}$ are derived in a similar way than it was performed for the upper bound. Consequently, constraints on the rate of change of input are incorporated into the optimisation problem through the matrix form

$$\underbrace{\begin{bmatrix} I \\ -I \end{bmatrix}}_{A_{\Delta u}} \underbrace{\begin{bmatrix} \Delta u_{0,0|k} \\ \Delta u_{0,1|k} \\ \vdots \\ \Delta u_{0,c-1|k} \end{bmatrix}}_{\mathbf{\Delta u_0}} \leq \underbrace{\begin{bmatrix} \overline{\Delta u} \\ \overline{\mathbf{\Delta u}} \\ -\underline{\Delta u} \\ -\underline{\mathbf{\Delta u}} \end{bmatrix} + \begin{bmatrix} \Delta u_{r,k} \\ \mathbf{0} \\ -\Delta u_{r,k} \\ \mathbf{0} \end{bmatrix}}_{\mathbf{b_{\Delta u}}} \quad (42)$$

with I as the identity matrix, $\underline{\mathbf{\Delta u}} \in \mathbb{R}^{(c-1)\times 1}$ and $\overline{\mathbf{\Delta u}} \in \mathbb{R}^{(c-1)\times 1}$ as vectors of repeated elements $\underline{\Delta u}$ and $\overline{\Delta u}$ respectively, and $\mathbf{0} \in \mathbb{R}^{(c-1)\times 1}$ as the zero vector.

Lastly, constraints (5) on output are introduced into the optimisation problem in the same fashion than the classical QDMC approach because the prediction vector (31) is dependent only on the current state vector $\mathbf{x}_k$ and past input $u_{0,k-1}$. Hence, defining $\bar{\mathbf{y}} \in \mathbb{R}^{p\times 1}$ and $\underline{\mathbf{y}} \in \mathbb{R}^{p\times 1}$ as vectors of p elements $\bar{y}$ and $\underline{y}$ respectively

$$\underbrace{\begin{bmatrix} G \\ -G \end{bmatrix}}_{A_y} \underbrace{\begin{bmatrix} \Delta u_{0,0|k} \\ \Delta u_{0,1|k} \\ \vdots \\ \Delta u_{0,c-1|k} \end{bmatrix}}_{\mathbf{\Delta u_0}} \leq \underbrace{\begin{bmatrix} \bar{\mathbf{y}} - \mathbf{y_{free}} \\ -\underline{\mathbf{y}} + \mathbf{y_{free}} \end{bmatrix}}_{\mathbf{b_y}}. \quad (43)$$

In summary, the optimisation problem for the modified predictive controller of the proposed loop is stated as (44) with constraints matrices defined in (37), (42), and (43).

$$\begin{aligned}
&\min_{\mathbf{\Delta u_0}} \left\{\|\mathbf{y_r} - \mathbf{y_f}\|_{\Gamma}^2 + \|\mathbf{\Delta u_0}\|_{\Lambda}^2\right\} \\
&\text{s.t.} \begin{bmatrix} A_{\Delta u} \\ A_u \\ A_y \end{bmatrix} \mathbf{\Delta u_0} \leq \begin{bmatrix} \mathbf{b_{\Delta u}} \\ \mathbf{b_u} \\ \mathbf{b_y} \end{bmatrix}
\end{aligned} \quad (44)$$

3.3. Stability and feasibility of the proposed control scheme

The closed-loop stability of the control architecture from Fig. 3 can be addressed based on the separation principle under which the disturbance rejector and the modified predictive controller constitute two cascaded systems that can be independently designed. If the stability of these two comprising structures is assured, then the closed-loop stability is guaranteed [27,28].

To illustrate the above, consider the following class of non-linear uncertain systems of relative order n, which can describe various practical systems.

$$\begin{aligned} \dot{\tilde{\mathbf{x}}}(t) &= A\tilde{\mathbf{x}}(t) + Bu(t) + B_f\left(\mathbf{h}\left(\tilde{\mathbf{x}}(t), u(t), t\right) + \mathbf{d}(t)\right) \\ y(t) &= C\tilde{\mathbf{x}}(t), \quad t \geq t_0 \end{aligned} \tag{45}$$

where $\tilde{\mathbf{x}}(t) \in \mathbb{R}^n$ is the state vector, $y(t) \in \mathbb{R}$ is the output, $u(t) \in \mathbb{R}$ is the control input, $\mathbf{d}(t) \in \mathbb{R}^m$ are possibly unknown time-varying and non-linear external disturbances, and $\mathbf{h}\left(\tilde{\mathbf{x}}(t), u(t), t\right) \in \mathbb{R}^m$ represents an unknown term including non-modelled dynamics and uncertainty. The matrices $A \in \mathbb{R}^{n\times n}$, $B \in \mathbb{R}^{n\times 1}$, $B_f \in \mathbb{R}^{n\times m}$, and $C \in \mathbb{R}^{1\times n}$ are the nominal system matrices.

Assumption 1. The non-linear system (45) has bounded domain $D_{\tilde{x}} \triangleq \left\{\tilde{\mathbf{x}}(t) : \|\tilde{\mathbf{x}}(t)\| < r_{\tilde{x}}\right\}$ $\forall t > 0$, $r_{\tilde{x}} > 0$.

Assumption 2. The external disturbance is bounded and has a bounded first-time derivative, i.e. $\|\mathbf{d}(t)\| < r_d$, $\|\dot{\mathbf{d}}(t)\| < r_{\dot{d}}$, $r_d, r_{\dot{d}} > 0$.

Assumption 3. The function $\mathbf{h}\left(\tilde{\mathbf{x}}(t), u(t), t\right)$ is continuously differentiable locally Lipschitz.

Under the active disturbance rejection framework, the system (45) can be reformulated as (46) [6,29], where dependence on continuous time has been omitted without loss of generality.

$$\begin{aligned} \dot{x}_1 &= x_2 \\ \dot{x}_2 &= -\frac{1}{\tau}x_2 + b_0 u + \underbrace{\frac{1}{\tau}x_2 + g\left(\tilde{\mathbf{x}}, \mathbf{h}, \mathbf{x}, \dot{\mathbf{h}}\right)}_{f} \\ y &= x_1 \end{aligned} \tag{46}$$

Notice that, with the formulation (46), the non-linear uncertain system (45) is transformed into a realisation of first-order plus integrator equivalent to (19) and whose dynamics is described only by the nominal value of the critical gain b_0 and the apparent time constant τ. This reformulation is the core of the ADRC. The remaining unknown terms are lumped in the total perturbation f to be estimated and compensated for via the extended state observer resulting in a disturbance-free linear modified plant.

Remark 1. The total perturbation is the conceptualisation of the total effect of multiple disturbances on the controlled variable, which combines the mismatch between the actual general non-linear model and the assumed first-order plus integrator system, besides the non-modelled or neglected dynamics lumped in the function g. The total perturbation is not necessarily a particular concrete disturbance. Moreover, under Assumptions $1-3$, f is continuously differentiable and bounded. A profound analysis of the conceptualisation of the total perturbation which lead to formulation (46) is found in [6].

Remark 2. The formulation of the control problem under the ADRC framework has been presented in the literature for different types of non-linear systems (e.g. in [27,30]). From this approach, the actual plant can be transformed into the assumed modified plant proposed in this work extending the applicability of the control scheme from Fig. 3 to a variety of linear and non-linear uncertain systems.

The total perturbation is treated as a function of time (regardless of its nature) reflected in the output. This is, the measured output contains sufficient information to estimate f [27]. As stated in Section 3.1, the estimation and rejection task is completed through the discrete ESO (21) based on the discrete realisation of (46), which is equivalent to the state–space (20) with y_k as the discrete measurements of y and u_k as the input combining the control action computed by the modified predictive controller and the compensation term.

Let $\mathbf{e}_k = \mathbf{x}_k - \hat{\mathbf{x}}_k$ be the discrete-time estimation error such that (47) is obtained by subtracting (21) from (20) and after some mathematical manipulation.

$$\mathbf{e}_{k+1} = \left(A_o - \boldsymbol{\ell}_o C_o A_o\right)\mathbf{e}_k. \tag{47}$$

Thus, the discrete ESO from the disturbance rejector is stable if the gains vector $\boldsymbol{\ell}_o$ is designed by assuring that matrix $A_o - \boldsymbol{\ell}_o C_o A_o$, representing the observation error dynamics, has all its eigenvalues inside the unit circle. This principle holds in gains (23)–(25), which, for a given b_0 and τ, depends only on the sampling time and the observer bandwidth. For a detailed presentation of the Input-to-State stability properties of the discrete ESO that establish the ultimate bounds for the estimation error, the reader is referred to [12]. Notice that the ESO comprising the proposed loop can be seen as a particular realisation of the discrete generalised ESO addressed in [12] in which the matrices are always defined by (22).

On the other hand, the asymptotic stability of the modified predictive controller can be assured by including a terminal constraint in the optimisation problem (44), such that the predicted outputs are forced to converge to the desired reference at the end of the prediction horizon and to remain at this setpoint for several desired additional instants. The use of a terminal equality constraint is one of the *ingredients* that characterise the type of predictive controllers that satisfy closed-loop asymptotic stability, being particularly the most straightforward option if the system to be controlled is linear, constrained and the problem of tracking a constant reference is considered [31,32].

For the above, consider the vector of additional n future outputs over the prediction horizon p

$$\tilde{\mathbf{y}}_f = \left[y_{f,p+1|k}, y_{f,p+2|k}, \ldots, y_{f,p+n|k}\right]^\top, \tag{48}$$

which is recursively computed as

$$\tilde{\mathbf{y}}_f = \underbrace{\widetilde{P}\hat{\mathbf{x}}_k + \widetilde{V}Bu_{0,k-1}}_{\tilde{\mathbf{y}}_{free}} + \widetilde{G}\boldsymbol{\Delta}\mathbf{u_0}, \tag{49}$$

with $\widetilde{P} \in \mathbb{R}^{n\times 2}$, $\widetilde{V} \in \mathbb{R}^{n\times 1}$, and $\widetilde{G} \in \mathbb{R}^{n\times c}$. Using this formulation, (44) is additionally subject to the equality constraint

$$\widetilde{G}\boldsymbol{\Delta}\mathbf{u_0} = \tilde{\mathbf{y}}_r - \tilde{\mathbf{y}}_f, \tag{50}$$

where $\tilde{\mathbf{y}}_r \in \mathbb{R}^{n\times 1}$ is a vector with all its components equal to the desired reference value $y_{r,p|k}$.

The approach in which a constraint in the form of (50) is included in the MPC optimisation problem is usually referred to in the literature as the Constrained Receding-Horizon Predictive Control (CRHPC) [33], and if (50) holds, then $y_{f,p+i|k} = y_{r,p|k}$ for $i = 1, 2, \ldots, n$, bringing a monotonically convergent cost and guaranteeing the closed-loop stability for finite horizons [34]. The number of additional n output predictions for which (50) is imposed is directly related to the system order. Therefore, for the modified predictive controller, $n = 2$ always as the prediction model is a fixed second-order state space realisation resembling the assumed modified plant of a first-order plus integrator and imposing this constraint on the optimisation problem results in the control horizon being selected according to $c \geq n = 2$, setting a lower bound for the tuning of c in the proposed constrained loop.

Notice that (44) can also include constraints on the rate of change of the manipulated variable, its magnitude, and the output. Imposing restrictions on predictive control can lead to feasibility problems. The optimiser may not find a solution that allows the system to be within the predefined conditions [22]. From an engineering perspective, a common approach is to soften the output constraints since they are often desired rather than required in contrast to the hard input constraints associated with physical limitations of the system, such as actuator ranges and slew rates [1]. Therefore, to deal with infeasibility, the cost index (29) of the modified predictive controller is reformulated as (51), where the last two terms penalise with the weight ε_1 the slack variable ξ_1 quantifying the violation of the output constraint, and through the weight ε_2 the slack variable ξ_2 associated to the equality constraint [35].

$$J_M = \sum_{i=1}^{p} \|y_{r,i|k} - y_{f,i|k}\|_\gamma^2 + \sum_{i=0}^{c-1} \|\Delta u_{0,i|k}\|_\lambda^2 + \sum_{i=1}^{p} \|\xi_{1,i|k}\|_{\varepsilon_1}^2 + \sum_{i=p+1}^{p+2} \|\xi_{2,i|k}\|_{\varepsilon_2}^2 \tag{51}$$

With the introduction of the slack variables and the stability constraint, the optimisation problem (44) is transformed in (52), where **0** and **1** are all-zeros and all-ones matrices of proper dimensions, respectively.

$$\begin{aligned} &\min_{\boldsymbol{\Delta u_0},\xi_1,\xi_2} \left\{\|\mathbf{y_r} - \mathbf{y_f}\|_\Gamma^2 + \|\boldsymbol{\Delta u_0}\|_\Lambda^2 + p\varepsilon_1\xi_1^2 + 2\varepsilon_2\xi_2^2\right\} \\ &\text{s.t.} \\ &\begin{bmatrix} A_{\Delta u} & \mathbf{0} & \mathbf{0} \\ A_u & \mathbf{0} & \mathbf{0} \\ A_y & -\mathbf{1} & 0 \\ \mathbf{0} & -1 & 0 \\ \mathbf{0} & 0 & 1 \end{bmatrix} \begin{bmatrix} \boldsymbol{\Delta u_0} \\ \xi_1 \\ \xi_2 \end{bmatrix} \le \begin{bmatrix} \mathbf{b_{\Delta u}} \\ \mathbf{b_u} \\ \mathbf{b_y} \\ 0 \\ \infty \end{bmatrix}; \\ &\begin{bmatrix} \widetilde{G} & \mathbf{0} & -\mathbf{1} \end{bmatrix} \begin{bmatrix} \boldsymbol{\Delta u_0} \\ \xi_1 \\ \xi_2 \end{bmatrix} = \tilde{\mathbf{y}}_r - \tilde{\mathbf{y}}_f \end{aligned} \tag{52}$$

In summary, the general design of the proposed scheme of Fig. 3 involves the disturbance rejector (21)–(25) and the modified predictive controller (52) (cf. (37), (42), (43)) for the control of linear or non-linear systems. It is claimed that the proposal procures the active disturbance rejection, feasibility and closed-loop nominal stability given the following conditions.

Condition 1. Given the nominal value of the critical gain b_0 and the apparent time constant τ, which resembles the desired dynamics of a first-order with integrator plant, the observer bandwidth $\omega_o > 0$ and the sampling time $T_s > 0$ exist such that the observer gains (23)–(25) satisfy $A_o - \boldsymbol{\ell}_o C_o A_o$ has all its eigenvalues inside the unit circle. Then, the estimation error is bounded and tunable by ω_o and T_s.

Condition 2. The weight γ of the prediction error and the weight λ of the control action rate are set such that $\gamma \ge 0$ and $\lambda \ge 0$.

Condition 3. The number of instants for which the equality constraint is imposed is $n = 2$, given the fixed state–space realisation of second-order assumed as the prediction model.

Condition 4. The control horizon satisfies the relation $c \ge n$.

Condition 5. The prediction horizon satisfies the relation $p \ge c$.

Condition 1 is related to the design of the disturbance rejector to enforce the actual system to behave like the assumed modified plant. Conditions $3 - 4$ result from the CRHPC adaptation to the proposed modified predictive controller and they follow the postulates and proofs given for *Theorem 7* from [34].

Remark 3. Formulation (52) seeks a feasible control action for the modified plant, leading future outputs to stabilise at a computed reference. It is emphasised that the proposed scheme is intended for systems with no nominal model or input–output processes where the output is the only controlled variable, in contrast to the feedback state MPC based on the control of the complete state vector.

Remark 4. In the assumed prediction model, the first state coincides with the output. Therefore, for the regulation problem (the reference is set to zero), the modified predictive controller meets the classical characterisation proposed by [36], which guarantees stability with a terminal equality constraint and satisfies the axioms postulated in [31]. In the case of setpoint tracking, the work of [34] also demonstrates that with constraint (50), the cost index decreases monotonically with time.

Remark 5. The avoidance of equality constraints has been discussed in the literature due to their possible effects on the optimal control problem. However, it is also stated that they are the simplest option in the regulation to a setpoint [32] and continue to attract the researchers attention, for example, in the development of data-driven MPC implementations [37]. Moreover, the equality and inequality constraints in the proposed scheme are handled through penalty functions for feasibility.

Finally, it is worth clarifying that the proposed control architecture can be implemented using the formulations (44) or (52) for the modified predictive controller. Suppose (44) is the one selected. In that case, the design relies on adequately setting the tuning parameters to obtain a closed-loop stable response according to the desired performance, as is the standard approach in the classical MPC and ADRC implementations. On the contrary, the optimisation problem (52) addresses the stability and feasibility challenges, which let the designer test a broader range of combinations of the predictive controller parameters, given that the disturbance rejector adequately compensates for the total perturbation.

4. Validation examples for the modified active disturbance rejection predictive control

In this section, the control architecture of Fig. 3, referred to hereafter as Modified Active Disturbance Rejection Predictive Control (MADRPC), is validated with different types of systems. The modified predictive controller operates under the formulation (52) in all cases. This is, the designs seek the desired performance while assuring feasibility and closed-loop stability.

Remark 6. As shown in Fig. 3, the proposed control combines the disturbance rejector mechanism of the ADRC with the receding horizon strategy of the MPC. This integration is done mainly by preserving the internal loop of the classical ADRC structure that includes the ESO together with the sum-gain configuration, through which the real dynamics is enforced to behave like the modified plant, and by redefining the optimisation problem constraints in the form of (37), (42), and (43) to directly incorporate the compensation term $u_{r,k}$. Consequently, with the proposed control strategy, the discrepancies between the real system and the assumed plant and the external disturbances are actively compensated in the loop relaxing the predictive controller modelling requirement to a second-order general integral system.

Also, the inclusion of the compensation term in the constraints definition aims at maintaining the controlled variable, manipulated variable (control action acting on the real plant), and rate of change of manipulated variable within the real constraints bands. The name MADRPC is motivated by the these characteristics.

Remark 7. From a practical application perspective, the MADRPC offers advantages in the control of systems with no identified model because the only modelling required information is the approximation of the control gain b_0 and the desired apparent time constant τ. As a result, the future outputs (31) are obtained with a fixed second-order state–space prediction model, and the size of the optimisation problem (44) (or (52)) is only dependent on the horizon lengths. Additionally, the control and system constraints can be included, and the closed-loop stability can be imposed through constraint (50). On the other hand, the MADRPC design requires selecting the classical parameters involved in the MPC design (prediction horizon, control horizon, cost function weightings) besides the ESO bandwidth ω_0 and the modified plant parameters (b_0, τ). These parameters should be appropriately selected for the trade-off among the performance requirements.

4.1. A classical problem of motion control

As first example, the MADRPC is implemented to control a DC motor. The design is described in detail, recalling the structures of the proposed control architecture.

Regarding Fig. 3, consider:

System: It is desired to control the shaft angle of a DC motor modelled as (53) [38] with parametric uncertainty for the static gain $\underline{K} = 2.5 - 20(\%)$, and for the apparent time constant $\overline{\tau} = 0.9 + 20(\%)$ (s). The goal is to produce shaft movements of about 15 (°) with no overshoot in approximately two seconds by manipulating the input voltage in the range $|u| \leq 24$ (V) and allowing input changes of $|\Delta u| \leq 5$ (V). A sampling time of $T_s = 0.05$ (s) is chosen.

$$G_M(s) = \frac{2.5}{s\,(0.9s+1)} \tag{53}$$

Disturbance rejector: As the loop sampling frequency is $\omega_s = 2\pi/T_s = 40\pi$ (rad/s), an ESO bandwidth of $\omega_o = 20$ (rad/s) is selected, following that the observer bandwidth should be five to ten times lower than the sampling frequency [39]. From (53), the nominal static gain is $K = 2.5$ and the nominal apparent time constant is $\tau = 0.9$. Therefore, $b_0 \approx K/\tau \approx 2.8$. As a remark, approximate values for τ and b_0 can be deduced from the open loop response because they represent natural characteristics of the plant. Indeed, a retuning of b_0 might be further needed [40].

Predictive controller: There are no specific rules for the computation of the horizons or the weighting matrices associated with the optimisation problem. However, some general guidelines based on practical experience have been suggested in the literature. For example, in [41] it is reported that a proper starting point for prediction horizon is $p = T_{\text{set}}/T_s$, with T_{set} as the open-loop settling time. In case of no self-regulatory plants, T_{set} could be roughly approximated as five times the time constant. On the other hand, it is well known that weighting factors should be selected according to the robustness or aggressiveness desired. For example, for a fixed γ, small values for λ lead to faster responses but with possible overshoot. Conversely, if λ increases, smoother inputs are achieved. For the problem at hand, $p = 40$, $c = 9$, $\gamma = 1$, $\lambda = 0.1$, $\varepsilon_1 = \varepsilon_2 = 10^5$.

As shown in Fig. 4, the MADRPC drives the shaft angle to the desired setpoints satisfying both the performance requirements and constraints. Furthermore, in the presence of model uncertainty ($\underline{K}$, $\overline{\tau}$), the disturbance rejector succeeds in compensating for the total perturbation allowing the MADRPC to produce an output response very similar to that of the nominal case (K, τ). The same is not true if the system is controlled by a constrained OF-MPC designed with the same parameters and full access to the states; the closed-loop response deteriorates because overshoot appears. A PID controller ($K_C = 1.6, T_I = 1, T_D = 0.9$) tuned with the SIMC rules [42] has been included in Fig. 4 as an alternative comparative controller. The MADRPC outperforms the PID in the presence of uncertainty while keeping the changes in input within the desired limits.

The functioning of the disturbance rejector can be validated through the step response of the modified plant [43]. This is, an input step applied instead of the governing control input u_0 in Fig. 3 should produce the open-loop response of the modified plant, which is expected to asymptotically change at a constant rate following the step response of the assumed first-order plus integrator system.

The above behaviour is presented in Fig. 5 for different values of the ESO bandwidth. The estimation of the first state $\hat{x}_1$ of the modified plant is plotted in Fig. 5(a) and its second state $\hat{x}_2$ is illustrated in Fig. 5(b). Notice that $\hat{x}_1$ and $\hat{x}_2$ are the estimations of the output and its rate of change. Consequently, $\hat{x}_1$ starts to follow a quadratic growth and then exhibits a linear tendency after approximately two times the time constant. This monotonic response drives $\hat{x}_2$ to a steady-state equal to the desired static gain.

On the other hand, the disturbance rejector accuracy is dependent on the ESO bandwidth. For a low observer bandwidth, for example, $\omega_o = 5$ (rad/s), there is a slight difference between the desired first-order plus integrator response and the modified plant output. However, as the bandwidth increases, the modified plant responses tend to be indistinguishable. With the selected ESO bandwidth $\omega_o = 20$ (rad/s), the MADRPC actively compensates for the real system uncertainty and the closed-loop output satisfies the desired performance.

Finally, Fig. 6 shows that the MADRPC satisfies the closed-loop stability constraint imposed while controlling the uncertain DC motor. Fig. 6(a) plots the sequences of $p + n$ future outputs computed at three different instants in the time window $t \in [0, 4]$. The predicted outputs settle at the desired setpoint of 15 (°) at the end of the prediction horizon of $p = 40$ instants and remain unchanged for the imposed $n = 2$ consequent instants. Moreover, the cost function exhibits a monotonic convergence to zero along the said time window, as seen in Fig. 6(b).

4.2. Linear benchmark systems: high-order systems

The proposed MADRPC is now validated through the control of two different linear examples resembling varied dynamics of common interest in literature, which are considered benchmark systems [44]. These are a fourth-order system with its pole spacing dependent on a parameter and a third-order plant with a right-hand plane zero or non-minimum phase behaviour. The case-study systems are listed in Table 1, together with the nominal values adopted here.

Table 1
Linear benchmark systems and its nominal values.

Benchmark system	Parameters
$G_F(s) = \frac{K}{(s+1)(\beta s+1)(\beta^2 s+1)(\beta^3 s+1)}$	$K = 1$ $\beta = 0.5$
$G_R(s) = \frac{1-\beta s}{(\tau s+1)^3}$	$\beta = 1$ $\tau = 1$

For comparison purposes, the OF-MPC and LADRC algorithms were also designed to control the aforementioned benchmark

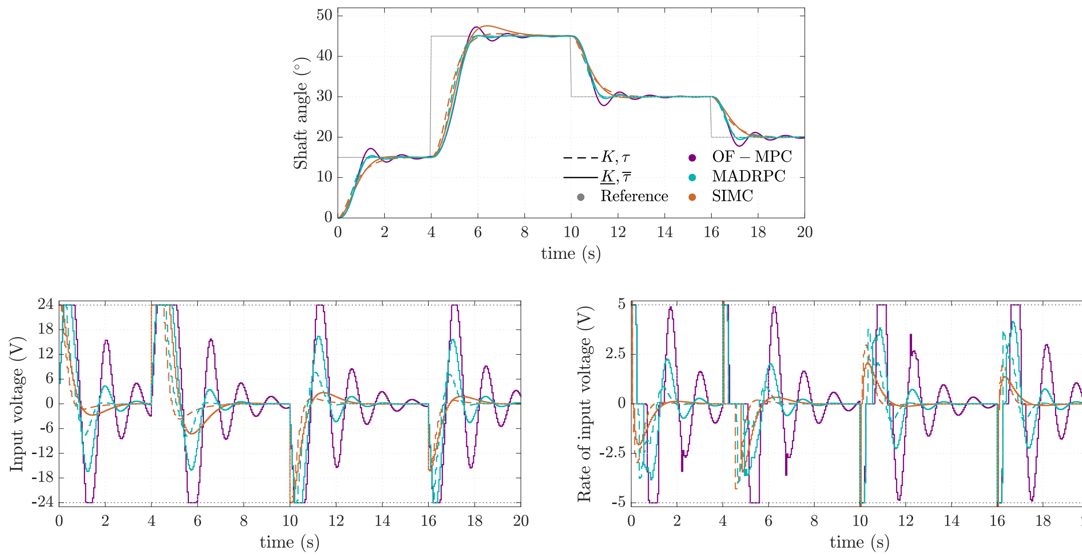

Fig. 4. Closed-loop response of the DC motor subject to PID-control, OF-MPC and MADRPC for different reference steps. Nominal system: K,τ; System with uncertainty: $\underline{K},\overline{\tau}$. System constraints: $|u|\ \leq\ 24$ (V), $|\Delta u|\ \leq\ 5$ (V), $y_{f,p+i|k}=y_{r,p|k},\ \ i\in[1,2]$.

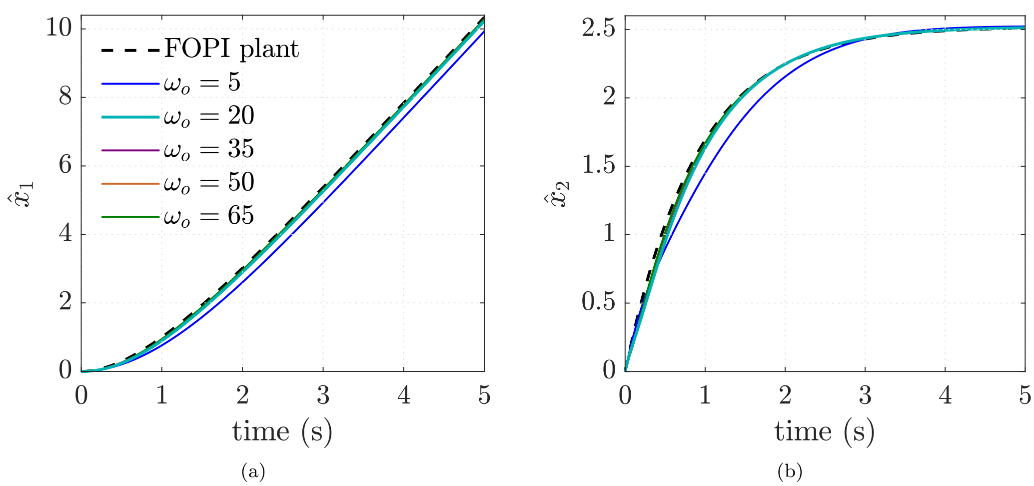

Fig. 5. Open-loop response of the modified plant of DC motor with uncertainty $\underline{K},\overline{\tau}$ under variations in the ESO bandwidth compared to the desired modified plant (FOPI, first-order plus integrator). (a) Estimated output. (b) Estimated rate of output.

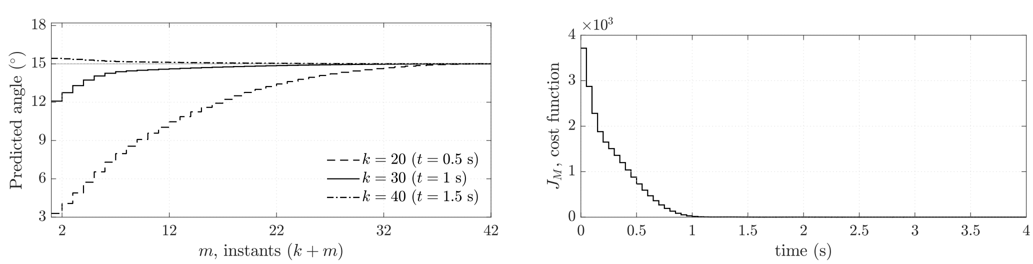

Fig. 6. Closed-loop stability validation of MADRPC when controlling the DC motor. (a). Equality constraint satisfaction $y_{f,p+i|k}\ =\ y_{r,p|k},\ \ i\ \in\ [1,2]$. (b). Monotonic convergence of the cost function.

systems. The OF-MPC, when no model mismatch exists, is considered a performance reference scheme because a complete, i.e. full-state model was used for its design. Therefore, the first validation objective was to test the MADRPC capability to emulate the OF-MPC performance with the advantage of a relaxation in the modelling requirement because of the disturbance rejector. On the other hand, it was expected that the MADRPC would outperform the conventional LADRC due to the modified prediction control law acting on the assumed modified plant.

As the MADRPC and LADRC algorithms use their corresponding ESO configurations, a current-type Luenberger observer of complete order was used to estimate the OF-MPC model states required for output predictions. To assign the same observer bandwidth of the ESO from MADRPC, the OF-MPC observer poles s_i were designed by solving the characteristic equation (54), which is only dependent on the system order n and desired bandwidth ω_o, and then mapped as z_i to the unit circle through (55) with

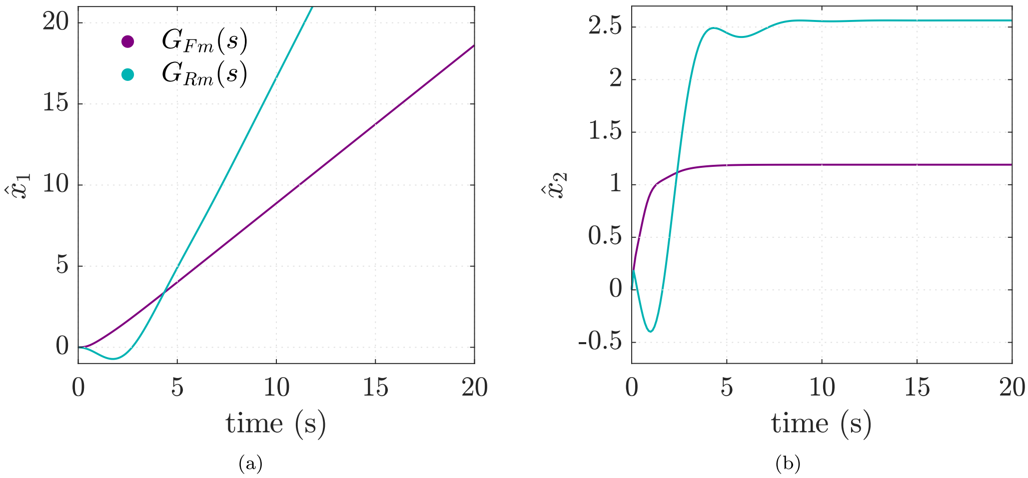

Fig. 7. Open-loop response of the modified plants $G_{Fm}(s)$ and $G_{Rm}(s)$ of the nominal linear benchmark systems from Table 1. (a) Estimated output. (b) Estimated rate of output.

Table 2
Control parameters for linear benchmark systems: p, prediction horizon; c, control horizon; γ, weighting for error; λ, weighting for rate of input; b_0, nominal critical gain; τ, apparent time constant; ω_o, ESO bandwidth; ω_c, controller bandwidth.

	$G_F(s)$			$G_R(s)$		
	LADRC	OF-MPC	MADRPC	LADRC	OF-MPC	MADRPC
p	–	50	50	–	85	85
c	–	10	5	–	20	20
γ	–	0.2	1	–	0.08	0.001
λ	–	1	0.1	–	1	5.5
b_0	25.68	–	2.4	10.37	–	4.5
τ	–	–	1	–	–	1.62
ω_o	23.20	5	5	9.6	12	12
ω_c	2.32	–	–	0.96	–	–

sampling time T_s.

$$\left(\frac{s}{\omega_o}\right)^{2n} = (-1)^{n+1} \tag{54}$$

$$z_i = \exp\left(s_i T_s\right) \tag{55}$$

The remaining parameters of the OF-MPC and MADRPC were selected as discussed in the previous example and according to the guidelines from [41]. In the case of the LADRC, the tuning rules from [45] were used to compute the main three design variables under the premise that first-order plus dead time models properly approximate the benchmark systems from Table 1, and thus, the parameters computed with the rules from [45] offers a stable closed-loop response with a medium robustness specification.

Table 2 gathers the design parameters for the three control algorithms. These control parameters were tuned considering that the main goal in servo operation, when possible, is to drive the system to the desired setpoint with an overshoot OS ≤ 2 % and a settling time $t_{98\%}$ lower than the natural pace of the system while constraints are satisfied. For this purpose, the control loops were designed with sampling time $T_s = 0.1$ (s).

As mentioned in Section 4.1, the open-loop response of the modified plant is an indicator of the ESO convergence and the MADRPC disturbance rejector capability to enforce the real plant to behave like the assumed dynamics. Therefore, a unit step input was applied to the modified plants corresponding to the nominal linear benchmark systems from Table 1. As can be seen in Fig. 7(a), the output of each modified plant resembles the desired dynamics of a first-order plus integrator model with the constant rate of change plotted in Fig. 7(b). The above shows that the disturbance rejector compensates for the ignored high-order dynamics; thus, the modified predictive controller can be designed to govern the assumed process.

Two scenarios were considered for validation. In the first one, the real plants to be controlled correspond to the nominal systems, and in the second one, the nominal parameters of each benchmark process were varied to test the designed control algorithms against uncertainty. Moreover, a step-type input disturbance was added to the manipulated variable in both scenarios at an instant when the output had reached the steady-state.

Quantification of performance was done through the indices reported in Table 3. For servo operation, settling time $t_{98\%}$ (s), percentage of overshoot OS (or absolute value of undershoot |US| in case of $G_R(s)$), and total variation of control action TV_s were computed. In contrast, the percentage of maximum deviation MD, ITAE, and total variation TV_d were calculated in regulatory operation.

The closed-loop responses of system $G_F(s)$ when controlled by LADRC, OF-MPC, and MADRPC are presented in Fig. 8. The MADRPC algorithm meets the required setpoint tracking performance and satisfy the constraints similarly to the OF-MPC. However, notice that in the first scenario, the OF-MPC has no model mismatch and complete state estimation. In contrast, the MADRPC manages to control the process assuming a fixed state–space realisation computed based on the values of the nominal critical gain and the apparent time constant. The MADRPC overcome the non-modelled dynamics and drives the output to the reference in a similar settling time to OF-MPC and with an overshoot within the desired band. Besides, the MADRPC reaches the setpoint in half of the time than the conventional LADRC.

During the second scenario, where the model mismatch is introduced, the OF-MPC holds the tracking performance at the cost of an increase in the total variation of the input, which is also reflected in the disturbance rejection response. Although the maximum deviations from the reference produced by the MADRPC are comparable with those produced for the OF-MPC, about 25%, the MADRPC returns the output to the steady state in less time and with a smoother variation in the control signal than the OF-MPC as reflected in the ITAE index. The disturbance rejection capability of the MADRPC also outperforms that of the LADRC.

On the other hand, Fig. 9 shows the closed-loop responses of system $G_R(s)$. In this case, the non-minimum zero produces an inverse response in the output. The OF-MPC leads the controlled

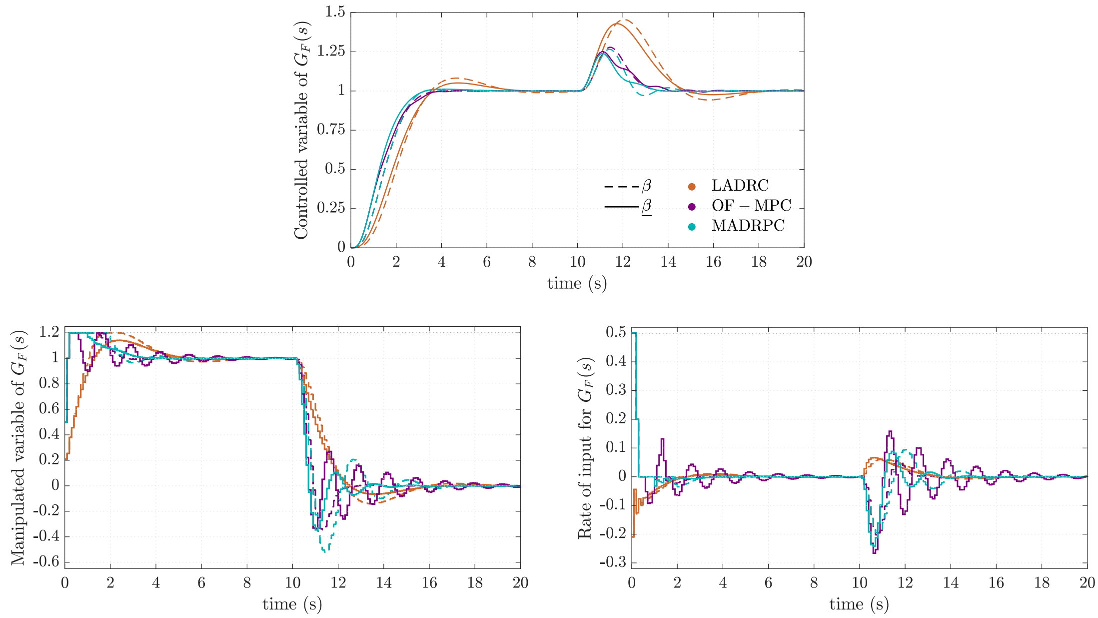

Fig. 8. Closed-loop response of $G_F(s)$ with LADRC, OF-MPC, and MADRPC. A step-type input disturbance is applied to the system at steady-state. System constraints: $|u| \leq 1.2$, $|\Delta u| \leq 0.5$, $y \leq 1.5$, $y_{f,p+i|k} = y_{r,p|k}$, $i \in [1, n]$.

Table 3
Performance indexes for the linear benchmark systems. The uncertainties $\overline{a}(b\%)$ and $\underline{a}(b\%)$ indicate that the parameter a was increased or decreased by b % of its nominal value, respectively.

Uncertainty	Controller	$G_F(s)$					
		$t_{98\%}$ (s)	OS (%)	TV_s	MD (%)	ITAE	TV_d
none	LADRC	6.4	8.2	1.25	46.13	3.30	1.32
	OF-MPC	3.2	0	0.91	27.86	0.68	1.70
	MADRPC	2.9	0.8	1.04	26.64	0.68	2.82
$\underline{\beta}(20\%)$	LADRC	6.3	5.1	1.09	43.22	2.49	1.14
	OF-MPC	3.4	0.5	2.35	25.24	0.74	4.20
	MADRPC	2.9	1.2	0.90	24.02	0.49	2.11
		$G_R(s)$					
Uncertainty	Controller	$t_{98\%}$ (s)	|US|	TV_s	MD (%)	ITAE	TV_d
none	LADRC	12.6	0.03	0.92	74.03	28.49	1.22
	OF-MPC	5.3	0.16	2.08	48.54	3.61	6.25
	MADRPC	7.7	0.05	1.23	69.95	13.43	1.71
$\overline{\beta}(20\%)$ $\underline{\tau}(2\%)$	LADRC	12.1	0.05	0.92	78.89	28.58	1.30
	OF-MPC	5.7	0.35	8.93	95.18	3.78	30.16
	MADRPC	9.4	0.08	1.28	79.85	14.50	2.10

variable to the reference in a time that results lower than the open-loop settling time of the process, even when there is a model mismatch. The MADRPC satisfies the desired overshoot, but the output is about 2 (s) slower than the response produced by the OF-MPC, although the MADRPC loop settles 5 (s) faster than LADRC in the nominal case.

The complete model information used within the OF-MPC aids this algorithm in the disturbance rejection performance resulting in lower deviations and ITAE indexes than those produced by the MADRPC and LADRC schemes in the absence of uncertainty. However, the MADRPC and LADRC offer a higher level of robustness in contrast to OF-MPC, which, for the model mismatch introduced, produces oscillations in the manipulated variable that worsen the inverse response and deteriorate both the servo and regulatory operation. The MADRPC offers better setpoint following and disturbance rejection than conventional LADRC, with the advantage that all constraints are directly taken into account in the computation of the control law.

4.3. Nonlinear benchmark system: The continuous stirred tank reactor

The Continuous Stirred Tank Reactor (CSTR) is considered a benchmark system in process control because it constitutes a vital unit operation, particularly in the chemical industry. The CSTR is often treated as a perfectly mixed module in which a first-order exothermic irreversible reaction occurs. This is, a fluid stream of reactant A is fed to the tank to be converted into product B with the same concentration and temperature as the reactor fluid [46]. As the reaction occurs, heat is generated and then must be removed with the aid of a coolant flowing through a jacket surrounding the reactor walls. According to the formulation of the mass and energy balance equations, the concentration can be controlled through the inlet flow rate. This scenario is analysed to validate the proposed MADRPC algorithm in the following. Additionally, the closed-loop performance is compared to OF-MPC and LADRC schemes.

A CSTR governed by the differential equations (56)–(57) [47] is considered. In this configuration, the controlled variable is the concentration of reactant A, C_A, and the manipulated variable is the coolant flow rate, q. The steady-state solution of the non-linear equations for a specific value of q leads to the operating points of the system. For example, with a coolant flow rate $q_0 =$ 103 (L/min), the concentration and temperature of reactor are correspondingly, $C_{Ao} = 0.09$ (mol/L) and $T_o = 438.77$ (K), which indicates states of high conversion and high release of energy. Description of variables and their corresponding nominal values for this example are listed in Table 4.

$$\dot{C_A} = \frac{F}{V}\left(C_{AF} - C_A\right) - k_0 C_A \exp\left(\frac{-E}{RT}\right) \tag{56}$$

$$\dot{T} = \frac{F}{V}\left(T_f - T\right) - \frac{\Delta H k_0 C_A}{\rho C_p} \exp\left(\frac{-E}{RT}\right) + q\frac{\rho_c C_{pc}}{\rho C_p V}\left[1 - \exp\left(\frac{-UA}{q\rho C_p}\right)\right]\left(T_c - T\right) \tag{57}$$

The system is open-loop stable around the selected operating point, as shown in Fig. 10. However, the non-linear dynamics become more evident as the coolant flow rate varies from its

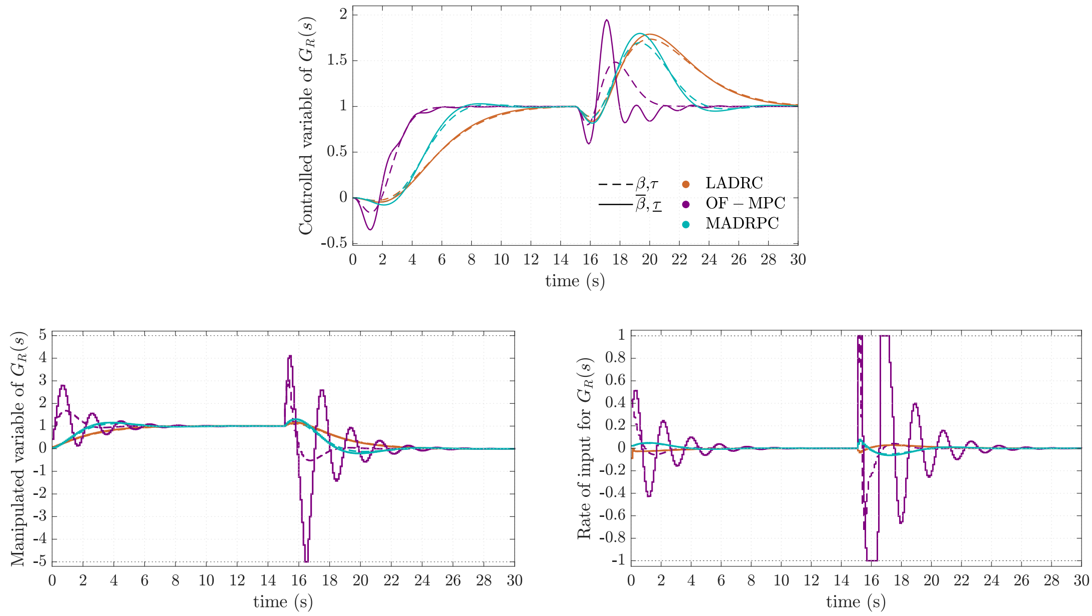

Fig. 9. Closed-loop response of $G_R(s)$ with LADRC, OF-MPC, and MADRPC. A step-type input disturbance is applied to the system at steady-state. System constraints: $|u| \leq 5$; $|\Delta u| \leq 1$; $y \leq 2$, $y_{f,p+i|k} = y_{r,p|k}$, $i \in [1, n]$.

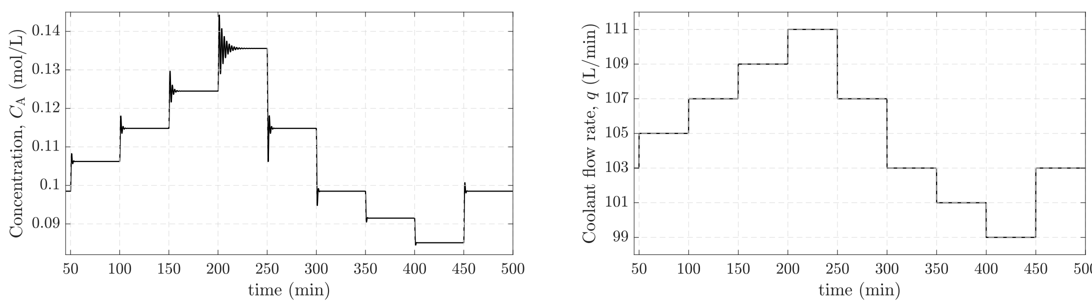

Fig. 10. Open-loop evolution of the concentration in product A, C_A, when the coolant flow rate q varies from its nominal value $q_o = 103$ (L/min). The highly nonlinear behaviour becomes more evident as the concentration reaches values far from the operating point $C_{Ao} = 0.09$ (mol/L).

Table 4
Description of variables and nominal values for control of the CSTR concentration.

Variable	Description	Nominal value
C_{AF}	Feed concentration	1 mol/L
V	CSTR volume	100 L
k_0	Reaction rate constant	7.2×10^{10} min^{-1}
E/R	Activation energy	1×10^4 K
ΔH	Heat of reaction	-2×10^5 Cal/mol
ρ, ρ_c	Liquid densities	1×10^3 g/L
C_p, C_{pc}	Specific heats	1 Cal/gK
UA	Heat transfer term	7×10^5 Cal/minK
F	Feed flow rate	100 L/min
T_f	Feed temperature	350 K
T_c	Coolant temperature	350 K
q_o	Coolant flow rate at the operating point	103 L/min
T_o	Reactor temperature at the operating point	438.77 K
C_{Ao}	Reactor concentration at the operating point	0.09 mol/L

nominal value producing an underdamped-type response in the reactor concentration. Therefore, the control goal is to drive the system such that the reactant concentration C_A follows the desired setpoint with no overshoot, allowing the coolant flow rate to operate in the range $80 \leq q \leq 115$ with changes $|\Delta q| \leq 1$.

The system was simulated with the three control algorithms: OF-MPC, the proposed MADRPC, and LADRC. For the OF-MPC design, (56)–(57) were linearised around the selected operating point ($C_{Ao} = 0.09$; $T_o = 438.77$; $q_o = 103$) and discretised with a sampling time $T_s = 0.083$ (min) [48]. The corresponding state–space model is (58) with $[x_1, x_2]^\top = [C_A, T]^\top$, $u = q$, and $y = C_A$.

$$\begin{aligned}\begin{bmatrix} x_{1,k+1} \\ x_{2,k+1} \end{bmatrix} &= \begin{bmatrix} 0.2248 & -0.00342 \\ 133.3 & 1.501 \end{bmatrix}\begin{bmatrix} x_{1,k} \\ x_{2,k} \end{bmatrix} + \begin{bmatrix} 1.3071 \times 10^{-4} \\ -0.0926 \end{bmatrix} u_k \\ y_k &= \begin{bmatrix} 1 & 0 \end{bmatrix}\begin{bmatrix} x_{1,k} \\ x_{2,k} \end{bmatrix}\end{aligned} \tag{58}$$

As the sampling rate is $\omega_s = 75.7$ (rad/min), a current observer with bandwidth $\omega_o = 15$ (rad/min) was designed to estimate the states of (58). These estimated states are used within the OF-MPC algorithm to predict the output along a prediction horizon $p = 29$ with a control horizon $c = 10$ and weighting coefficients $\gamma = 2.22$ and $\lambda = 0.05$. As in the previous validation examples, the OF-MPC algorithm was implemented with the operating constraints, the equality constraint to assure stability and their corresponding slack variables with weights $\varepsilon_1 = \varepsilon_2 = 10^5$.

On the other hand, the disturbance rejector of the MADRPC was designed as follows: the values of the apparent time constant τ and nominal critical gain b_0 were deduced from the open-loop response. As shown in Fig. 10, for input changes of 2 (min/L), the reactant concentration varies approximately in 0.01 (mol/L) with a mean settling time of 5 (min). Therefore, the modified plant parameters were set as $\tau = 1$ (min) and $b_0 = 0.03$ (mol/minL).

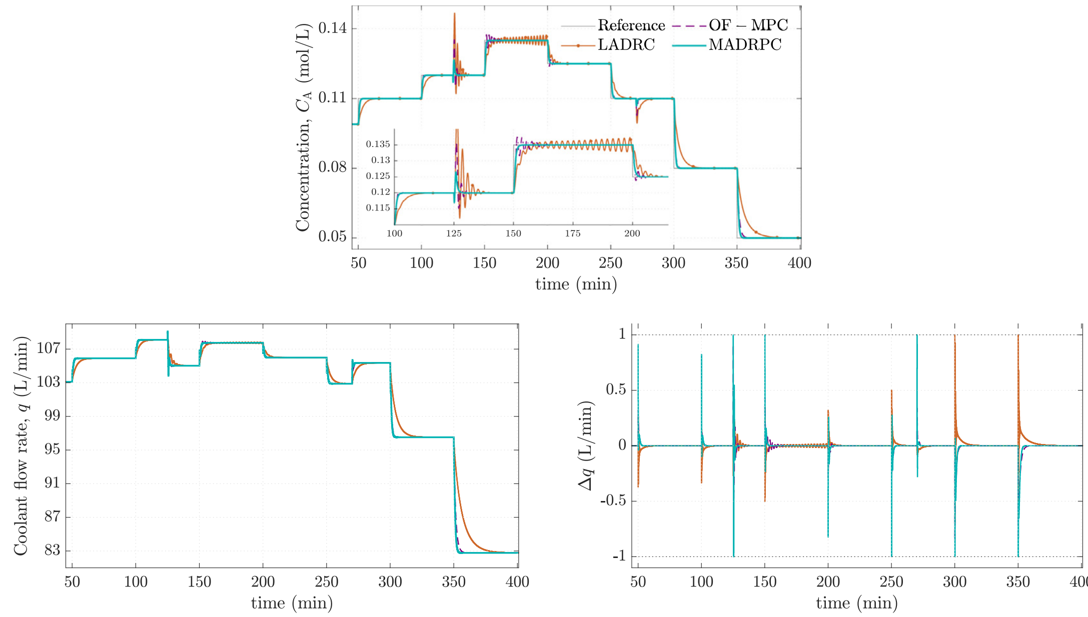

Fig. 11. Closed-loop response of the CSTR with LADRC, OF-MPC, and MADRPC. System constraints: $80 \leq q \leq 115$; $|\Delta q| \leq 1$; $C_{Af,p+i|k} = C_{Ar,p|k}$, $i \in [1, 2]$.

The ESO bandwidth was chosen as $\omega_o = 15$ (rad/min), and the modified predictive controller parameters were designed as $p = 29$, $c = 15$, $\gamma = 10$, $\lambda = 0.001$, and $\varepsilon_1 = \varepsilon_2 = 10^5$.

Finally, for the LADRC design, the same bandwidth $\omega_o = 15$ (rad/min) was selected for the ESO, the controller bandwidth was set as $\omega_c = 10$ (rad/min), and the nominal value of control gain had to be tuned to $b_0 = 3$ (mol/minL) for the system to be closed-loop stable.

The closed-loop response of the CSTR is presented in Fig. 11. A multi-step reference was applied to the system to test the dynamic behaviour when the concentration C_A is required to increase or decrease from its nominal value. What is more, uncertainty was included in the process at $t = 125$ (min), reducing the concentration feed and increasing the reaction rate constant by 2% of its corresponding nominal values, and at $t = 270$ (min) when the coolant temperature was increased from 350 (K) to 352 (K).

According to the performance indices from Table 5, the MADRPC follows the desired setpoints with no overshoot and a settling time inferior to 3 (min) when the reference values are over the nominal concentration. The loop becomes slower for setpoints under C_{Ao}, but the MADRPC algorithm is still the fastest.

Notice that the OF-MPC and LADRC produce an oscillating behaviour (referred to as Osc. in Table 5) when the reference is increased from 0.12 to 0.135, as seen in the inset of the concentration from Fig. 11. Although the OF-MPC manages to settle the output in the desired value, the detriment in the response is also present at the beginning of the next transient when C_A decreases to 0.125 causing that the system reaches the steady state with overshoot. The above exhibits the dependence of the OF-MPC on an accurate model, especially in the operating regions where the non-linear behaviour is more prominent, and the limitations of the LADRC to overcome such difficult dynamics.

With the selected tuning parameters, the MADRPC algorithm is also superior in terms of disturbance rejection. For example, the inset from Fig. 11 also shows the response of the three algorithms to the first alteration in the operating conditions at $t = 125$ (min). The MADRPC returns the concentration to the reference level producing the lowest deviation and the fastest response, as evidenced by the ITAE index. This rapid disturbance rejection increases the total variation of the coolant flow rate. However, the algorithm computes control actions that satisfy the given operation constraints.

5. Conclusions

In this paper, the Modified Active Disturbance Rejection Predictive Control (MADRPC) has been developed. The MADRPC is a discrete-time algorithm that merges the estimation–rejection capability of the ADRC with the receding horizon feature of the MPC. A current-type ESO is designed such that the real plant dynamics is enforced into a modified plant of first-order plus integrator. As a result, a predictive control law is computed based on a state-space realisation of second order with only two model parameters: the apparent time constant and the nominal value of control gain. Likewise, the control law results from an optimisation problem where constraints on decision variables are redefined to include the contribution of the perturbation compensation term to the manipulated variable, and the conditions for feasibility and nominal closed-loop stability has been established.

One significant advantage of the MADRPC is that the modelling requirement is relaxed because only information of two parameters is required, in contrast to conventional state–space MPC, which is highly dependent on a properly-identified model. By assuming a first-order plus integrator as the modified plant, the prediction model order is fixed. Therefore, the size of the optimisation problem related to the computation of the predictive control law exclusively depends on the horizons lengths.

Based on the validation results obtained, it can be concluded that the disturbance rejector of the MADRPC actively compensates for the total perturbation. Therefore, with the proposed control scheme is possible to achieve similar performance to that obtained with the MPC that uses a known linearised model of complete-order, a correction term, and constant state disturbance predictions to provide offset-free control. Furthermore, the MADRPC showed to be more robust than OF-MPC and conventional LADRC when it was used to operate a CSTR unit in regions of prominent non-linear dynamics offering proper servo-regulatory performance while satisfying constraints.

The MADRPC parameters selection was briefly discussed in this paper and the general guidelines presented were sufficient for the tuning of the reported case studies. Still, future work can be directed towards the MADRPC parameter tuning taking into account the trade-off between different performance objectives. Another research line goes with the direct extension of the

Table 5
Performance indexes for control of CSTR concentration.

Setpoint	Settling time (min)			Overshoot (%)			Total variation		
	LADRC	OF-MPC	MADRPC	LADRC	OF-MPC	MADRPC	LADRC	OF-MPC	MADRPC
0.09 to 0.11	12.53	3.24	2.74	0	0	0	3.93	2.80	2.87
0.11 to 0.12	11.29	3.15	2.66	0	1.18	0	3.23	2.22	2.60
0.12 to 0.135	Osc.	13.20	2.57	Osc.	16.10	0	Osc.	5.41	4.08
0.135 to 0.125	12.45	5.81	2.66	0.53	11.62	0	2.86	2.14	3.23
0.125 to 0.11	11.45	3.07	2.74	0	0.13	0	4.71	3.11	4.48
0.11 to 0.08	16.27	3.90	3.07	0	0	0	11.92	8.84	8.97
0.08 to 0.05	25.23	5.98	3.65	0	0	0	16.70	13.75	13.75
Time (min)	Max. deviation (%)			ITAE			Total variation		
125 to 150	22.24	12.81	5.40	0.18	0.03	0.01	5.96	7.35	9.33
270 to 300	9.69	6.78	2.86	0.11	0.01	0.003	2.47	2.48	4.04

MADRPC to MIMO systems. In this case, each manipulated channel could be treated as the first order plus integrator modified plant fixing the assumed dynamics for each channel.

Declaration of competing interest

The authors declare that they have no known competing financial interests or personal relationships that could have appeared to influence the work reported in this paper.

Acknowledgements

This work has been supported by MCIN/AEI/10.13039/501100011033 [Project PID2020-120087GB-C21], MCIN/AEI/10.13039/501100011033 [Project PID2020-119468RA-I00], the Generalitat Valenciana regional government, Spain [Project CIAICO/2021/064], and the Ministry of Science, Technology and Innovation of Colombia [scholarship programme 885].

References

[1] Schwenzer M, Ay M, Bergs T, Abel D. Review on model predictive control: An engineering perspective. Int J Adv Manuf Technol 2021;117:1327–49.
[2] Samad T, Bauer M, Bortoff S, Cairano SD, Fagiano L, Odgaard PF, et al. Industry engagement with control research: Perspective and messages. Annu Rev Control 2020;49:1–14.
[3] Domański PD. Performance assessment of predictive control—a survey. Algorithms 2020;13(4):97.
[4] Gao Z. Scaling and bandwidth-parameterization based controller tuning. In: Proceedings of the 2003 american control conference, 2003. Denver, CO, USA: IEEE; 2003, p. 4989–96.
[5] Han J. From PID to active disturbance rejection control. IEEE Trans Ind Electron 2009;56(3):900–6.
[6] Chen S, Bai W, Hu Y, Huang Y, Gao Z. On the conceptualization of total disturbance and its profound implications. Sci China Inf Sci 2019;63(2):129201.
[7] Wu Z, Gao Z, Li D, Chen Y, Liu Y. On transitioning from PID to ADRC in thermal power plants. Control Theory Technol 2021;19(1):3–18.
[8] Łakomy K, Madonski R, Dai B, Yang J, Kicki P, Ansari M, et al. Active disturbance rejection control design with suppression of sensor noise effects in application to DC–DC buck power converter. IEEE Trans Ind Electron 2022;69(1):816–24.
[9] Fareh R, Khadraoui S, Abdallah MY, Baziyad M, Bettayeb M. Active disturbance rejection control for robotic systems: A review. Mechatronics 2021;80:102671.
[10] Li S, Yang J, Chen W-H, Chen X. Generalized extended state observer based control for systems with mismatched uncertainties. IEEE Trans Ind Electron 2012;59(12):4792–802.
[11] Liu C, Negenborn RR, Zheng H, Chu X. A state-compensation extended state observer for model predictive control. Eur J Control 2017;36:1–9.
[12] Castillo A, Santos TL, Garcia P, Normey-Rico JE. Predictive ESO-based control with guaranteed stability for uncertain MIMO constrained systems. ISA Trans 2021;112:161–7.
[13] Liu H, Lin W, Liu Z, Buccella C, Cecati C. Model predictive current control with model-aid extended state observer compensation for PMSM drive. IEEE Trans Power Electron 2023;38(3):3152–62.
[14] Zhao Y, Liu H, Ding C, Cheng Y, Shurafa MAA, Wu J, et al. Research on MPDPC with FADRC control strategy for three-phase rectifying converter. Meas Control 2022;55(7–8):757–66.
[15] Li G, Madonski R, Lakomy K, Sun L, Lee KY. Extended state observer-based model predictive temperature control of mechanically pumped two-phase loop: An experimental study. Appl Therm Eng 2022;213:118663.
[16] Yang J, Cui H, Li S, Zolotas A. Optimized active disturbance rejection control for DC-DC buck converters with uncertainties using a reduced-order GPI observer. IEEE Trans Circuits Syst I: Reg Pap 2018;65(2):832–41.
[17] Suhail SA, Bazaz MA, Hussain S. MPC based active disturbance rejection control for automated steering control. Proc Inst Mech Eng D 2021;235(12):3199–206.
[18] Chen Z, Li Y, Sun M, Zhang Q, Sun Q. ADRC-GPC control of quad-rotor unmmaned aerial vehicle. J Harbin Inst Technol 2016;48(9):176–80, (In Chinese).
[19] Wu X, Li Y, Chen Z, Sun M. On the design and realization of active disturbance rejection generalized predictive control. IMA J Math Control Inform 2019;36(4):1275–304.
[20] Ren J, Chen Z, Sun M, Sun Q. Frequency performance analysis of proportional integral-type active disturbance rejection generalized predictive control for time delay systems. Syst Sci Control Eng 2021;10(1):1–14.
[21] Tatjewski P. Disturbance modeling and state estimation for offset-free predictive control with state-space process models. Int J Appl Math Comput Sci 2014;24(2):313–23.
[22] Maciejowski JM. Predictive control with constraints. 1st ed.. Boston: Addison-Wesley Educational; 2001.
[23] Miklosovic R, Radke A, Gao Z. Discrete implementation and generalization of the extended state observer. In: 2006 american control conference. Minneapolis, MN, USA: IEEE; 2006, p. 2209–14.
[24] Herbst G. A simulative study on active disturbance rejection control (ADRC) as a control tool for practitioners. Electronics 2013;2(4):246–79.
[25] Gao Z. On the centrality of disturbance rejection in automatic control. ISA Trans 2014;53(4):850–7.
[26] Madoński R, Herman P. Survey on methods of increasing the efficiency of extended state disturbance observers. ISA Trans 2015;56:18–27.
[27] Feng H, Guo B-Z. Active disturbance rejection control: Old and new results. Annu Rev Control 2017;44:238–48.
[28] Guerrero-Castellanos JF, González-Romeo LL. Position control system via active disturbance rejection for laser optical systems. Revista Iberoamericana de Automática e Informática Ind 2022;19(1):61–73.
[29] Chen S, Bai W. Performance analysis of typical linear augmented observers for a class of MIMO systems with nonlinear uncertainty. ISA Trans 2022;128:316–27.
[30] Huang Y, Xue W. Active disturbance rejection control: Methodology and theoretical analysis. ISA Trans 2014;53(4):963–76.
[31] Mayne D, Rawlings J, Rao C, Scokaert P. Constrained model predictive control: Stability and optimality. Automatica 2000;36(6):789–814.
[32] Rawlings JB, Mayne DQ. Model predictive control: theory and design. 1st ed.. Madison: Nob Hill Publishing; 2009.
[33] Clarke D. Advances in model-based predictive control. London, England: Oxford University Press; 1994.
[34] Yoon T-W, Clarke DW. A reformulation of receding-horizon predictive control. Internat J Systems Sci 1995;26(7):1383–400.
[35] Kerrigan EC, Maciejowski JM. Soft constraints and exact penalty functions in model predictive control. In: Proceedings of the UKACC international conference. 2000, p. 1–6.
[36] Keerthi SS, Gilbert EG. Optimal infinite-horizon feedback laws for a general class of constrained discrete-time systems: Stability and moving-horizon approximations. J Optim Theory Appl 1988;57(2):265–93.
[37] Berberich J, Kohler J, Muller MA, Allgower F. Data-driven model predictive control with stability and robustness guarantees. IEEE Trans Automat Control 2021;66(4):1702–17.
[38] Camacho E, Bordons C. Model predictive control. 1st ed.. London: Springer; 2007.
[39] Zhao S, Gao Z. Modified active disturbance rejection control for time-delay systems. ISA Trans 2014;53(4):882–8.

[40] Martínez BV, Sanchis J, García-Nieto S, Martínez M. Active disturbance rejection control: A guide for design and application. Revista Iberoamericana de Automática e Informática Ind 2021;18(3):201–17.
[41] Alhajeri M, Soroush M. Tuning guidelines for model-predictive control. Ind Eng Chem Res 2020;59(10):4177–91.
[42] Skogestad S, Grimholt C. The SIMC method for smooth PID controller tuning. In: Vilanova R, Visioli A, editors. PID control in the third millennium: lessons learned and new approaches. London: Springer London; 2012, p. 147–75.
[43] Sun L, Zhang Y, Li D, Lee KY. Tuning of active disturbance rejection control with application to power plant furnace regulation. Control Eng Pract 2019;92:104122.
[44] Åström K, Hägglund T. Benchmark systems for PID control. IFAC Proc Vol 2000;33(4):165–6.
[45] Martínez BV, Sanchis J, García-Nieto S, Martínez M. Tuning rules for active disturbance rejection controllers via multiobjective optimization—a guide for parameters computation based on robustness. Mathematics 2021;9(5):517.
[46] Bequette BW. Process dynamics. Philadelphia, PA, USA: Prentice Hall; 1998.
[47] Henson MA, Seborg DE. Input-output linearization of general nonlinear processes. AIChE J 1990;36(11):1753–7.
[48] Bhadra S, Panda A, Bhowmick P, Goswami S, Panda RC. Design and application of nonlinear model-based tracking control schemes employing DEKF estimation. Optim Control Appl Methods 2019;40(5):938–60.